

# Uspostava kulture i biološko oslikavanje organoida mišjeg tankog crijeva

---

**Kodba, Snježana**

**Master's thesis / Diplomski rad**

**2020**

*Degree Grantor / Ustanova koja je dodijelila akademski / stručni stupanj:* **University of Zagreb, Faculty of Science / Sveučilište u Zagrebu, Prirodoslovno-matematički fakultet**

*Permanent link / Trajna poveznica:* <https://um.nsk.hr/um:nbn:hr:217:490054>

*Rights / Prava:* [In copyright](#)/[Zaštićeno autorskim pravom.](#)

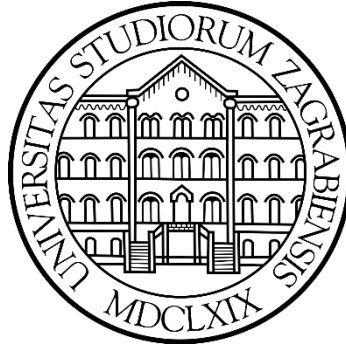
*Download date / Datum preuzimanja:* **2024-08-07**



*Repository / Repozitorij:*

[Repository of the Faculty of Science - University of Zagreb](#)





UNIVERSITY OF ZAGREB  
FACULTY OF SCIENCE  
DEPARTMENT OF BIOLOGY

Snježana Kodba

**ESTABLISHMENT AND BIO-IMAGING OF MOUSE SMALL INTESTINE  
ORGANOIDS CULTURE**

Graduation thesis

Zagreb, 2020.



This thesis was done in the Laboratory of Cell Biophysics, Division of Molecular Biology, Ruđer Bošković Institute, under the mentorship of prof. dr. Iva Tolić (Division of Molecular Biology, Ruđer Bošković Institute, 10000 Zagreb, Croatia). It is submitted to the Division of Biology, Faculty of Science to be evaluated to obtain the master's degree in molecular biology. Work in this thesis was supported by European Research Council (ERC).

## Acknowledgments

First, I would like to give special thanks to my mentor Iva Tolić, for all the opportunities you have given me and for broadening my scientific perception. Thank you for your advices and for all knowledge and skills I have gained under your mentorship.

Next, I would like to thank Kruno for helping me out when things were at dead end. Thank you for finding time to thoroughly examine the subject and helping me solve all the problems.

Moreover, I would like to thank Geert Kops for giving me the opportunity to gain all the necessary skills to get through this thesis; for all the help and advices which enabled me to finish my project.

Thanks are due to Joana and Pim who lead me through every step of the protocol, gave me many advices whenever I encountered a problem. Thank you for your help during my internship in Netherlands, but also for all your efforts to help me while I was in Croatia, trying things on my own.

I would like to thank Ivana Š. for all the support and encouragement during my time in the lab. Thank you for always making me see the solution to every problem.

Furthermore, I would like to thank Patrik for introducing me with all the lab work and helping me get through my first days in the lab.

I would like to thank Martina for help with MatLab and all late-night discussions.

I would like to thank members of Tolić group for scientific and non-scientific debates and for making my time in the lab more pleasant.

I would also like to thank members of Nenad Pavin group for showing me how molecular biology can be combined with theoretical physics.

Moreover, I would like to thank members of Kops group for making my internship a fulfilled experience and for many useful scientific discussions.

I would like to thank Iva Bazina and Mirela Baus Lončar for sacrificing mice for the purposes of this thesis.

Furthermore, I would like to thank Dragomira Majhen for allowing me to work in her lab when I encountered technical difficulties.

Moreover, I would like to thank my parents, sister, brothers, and friends for their constant support through my entire life and education. At last, I am thankful to Jurica, for enduring all my ups and downs, and for never letting me give up.

## TEMELJNA DOKUMENTACIJSKA KARTICA

---

Sveučilište u Zagrebu

Prirodoslovno-matematički fakultet

Biološki odsjek

Diplomski rad

Uspostava kulture i biološko oslikavanje organoida mišjeg tankog crijeva

Snježana Kodba

Rooseveltov trg 6, 10000 Zagreb, Hrvatska

Organoidi su novo područje u molekularnoj biologiji koje ima veliki potencijal u temeljnim i primijenjenim istraživanjima. Minijaturni organi uzgajani *in vitro* značajno nalikuju svojim nativnim dvojnicima u svim fiziološkim, 3D strukturalnim i anatomskim karakteristikama. Već je razvijeno više tipova organoida, uključujući ljudske i mišje organoide tankog crijeva. U ovom radu, ja sam uspješno uzgojila i održala u kulturi organoide mišjeg tankog crijeva. Nakon optimizacije, uzgojeni su organoidi mogli neodređeno dugo rasti i propagirati se u kulturi. Preciznija karakterizacija anatomije i morfologije organoida napravljena je nakon imunofluorescencijskog bojanja i biološkog oslikavanja. Nadalje, razvila sam novi protokol za imunofluorescencijsko bojanje cističnih, šupljih tipova organoida. U odnosu na literaturno dostupne protokole, novi protokol predstavlja poboljšanja u brzini izvedbe i broju koraka koji štede vrijeme i novac. Također, rezultati su pokazali da organoidi mišjeg tankog crijeva mogu dolaziti u različitim oblicima pri čemu veličina stanica unutar organoida ovisi o točnoj poziciji stanice u organoidu te o njihovom proliferacijskom statusu. Na kraju, stopa proliferacije organoida mišjeg tankog crijeva pada s povećanjem broja dana koje su organoidi proveli u kulturi. Zaključno, uspješno je razvijen protokol za izolaciju i uzgoj složenog sustava organoida iz mišjeg tankog crijeva koji ima potencijal brze optimizacije za korištenje na organoidima drugih organskih sustava.

(60 stranica, 51 slika, 35 literaturnih navoda, jezik izvornika: engleski)

Ključne riječi: organoidi, tanko crijevo, miš, mikroskopija

Voditelj: dr.sc. Iva Tolić

## BASIC DOCUMENTATION CARD

---

University of Zagreb

Faculty of Science

Department of Biology

Graduation thesis

Establishment and bio-imaging of mouse small intestine organoids culture

Snježana Kodba

Rooseveltova trg 6, 10000 Zagreb, Croatia

A novel field arising in molecular biology, organoids, have a great potential in basic and applied research. Mini organs grown in a dish remarkably resemble their native counterparts in almost every aspect of their physiological, 3D structural and anatomical properties. Many different types of organoids have yet been developed, including mouse and human small intestine organoids. In this thesis, I have successfully established and maintained a culture of mouse small intestine organoids. After some optimization was done, the organoids were able to keep growing and differentiating indefinitely. More precise characterization of their anatomy and morphology was made after immunofluorescent staining and bio-imaging. I have created a novel protocol for immunostaining of cystic, hollow types of the organoids which reduces the time and money consumed. The results have revealed different shapes of small intestine organoids and variation in cell size depending on the position and proliferation status. The proliferation rate, however, decreases as the days in culture increase. To conclude, a novel protocol for isolation and propagation of complex organoid system was successfully developed from mouse small intestine. However, it has potential for fast optimization and adjustment for other types of mouse and human organoids.

(60 pages, 51 figures, 35 references, original in English)

Key words: organoids, small intestine, mouse, microscopy

Supervisor: dr.sc. Iva Tolić



## Table of content

<b>Introduction .....</b>	<b>1</b>
<b>1.1. Historical review.....</b>	<b>1</b>
<b>1.1.1. Tumor cell line.....</b>	<b>1</b>
<b>1.1.2. Normal cell line.....</b>	<b>2</b>
<b>1.1.3. Organoids.....</b>	<b>2</b>
<b>1.2. 1. Organoids derived from PSCs.....</b>	<b>3</b>
<b>1.2.2. Organoids derived from ASCs .....</b>	<b>4</b>
<b>1.3. Stem cells .....</b>	<b>6</b>
<b>1.4. Small intestine: development, structure, and function .....</b>	<b>7</b>
<b>1.5. The need for small intestine organoids.....</b>	<b>10</b>
<b>1.6. Growth factors and signaling .....</b>	<b>11</b>
<b>1.7. Therapeutic potential of the organoids.....</b>	<b>13</b>
<b>1.8. The research aims.....</b>	<b>14</b>
<b>Materials and methods.....</b>	<b>15</b>
<b>2.1. Thawing of cryovial with small intestine organoids .....</b>	<b>15</b>
<b>2.2. Mouse small intestine isolation.....</b>	<b>15</b>
<b>2.3. Isolation of the intestinal crypts .....</b>	<b>19</b>
<b>2.4. Seeding small intestine crypts.....</b>	<b>21</b>
<b>2.5. Small intestine organoids splitting .....</b>	<b>23</b>
<b>2.6. Seeding small intestine organoids for immunolabeling.....</b>	<b>23</b>
<b>2.7. Fixation and blocking.....</b>	<b>24</b>
<b>2.8. Immunolabeling.....</b>	<b>24</b>
<b>2.9. DAPI and Phalloidin staining.....</b>	<b>25</b>
<b>2.10. Microscopy .....</b>	<b>26</b>
<b>2.11. Image and data analysis.....</b>	<b>26</b>
<b>2.12. Organoids morphology characterization .....</b>	<b>27</b>
<b>2.13. Cell size measurements .....</b>	<b>29</b>
<b>2.14. Cell proliferation determination .....</b>	<b>30</b>
<b>Results .....</b>	<b>33</b>
<b>3.1.1. Cryovial 1 .....</b>	<b>33</b>
<b>3.1.2. Cryovial 2 .....</b>	<b>33</b>
<b>3.1.3. Cryovial 3 .....</b>	<b>33</b>
<b>3.2.1. Mouse 1.....</b>	<b>34</b>
<b>3.2.2. Mouse 2.....</b>	<b>35</b>
<b>3.2.3. Mouse 3.....</b>	<b>35</b>
<b>3.3. Efficiency of immunolabeling.....</b>	<b>36</b>
<b>3.4. Different morphology of the mouse small intestine organoids .....</b>	<b>40</b>

<b>3.5. Small intestine is a hollow organ.....</b>	<b>41</b>
<b>3.6. Cells vary in size in small intestine organoids.....</b>	<b>44</b>
<b>3.7. Cell viability in small intestine organoids .....</b>	<b>48</b>
<b>Discussion.....</b>	<b>51</b>
<b>Conclusion.....</b>	<b>57</b>
<b>Literature .....</b>	<b>58</b>
<b>Curriculum vitae .....</b>	<b>61</b>

## **Abbreviations**

ASCs – adult stem cells

BSA – bovine serum albumin

CBC – crypt base columnar (cells)

CCM – crypt culture medium

EEC – enteroendocrine cells

EGF – epithelial growth factor

ES – embryonic stem (cells)

Fzd – frizzled (receptor)

ICM – intestinal culture medium

IEC – intestinal epithelial cells

IPS – induced pluripotent stem (cells)

Lgr5<sup>+</sup> – leucine-rich repeat-containing G-protein coupled receptor 5

OBM – organoid basal medium

PBS – phosphate buffer solution

PSCs – pluripotent stem cells

RT – room temperature

## Introduction

### 1.1. Historical review

#### 1.1.1. Tumor cell line

First human cell line successfully developed for long term use was HeLa cells (figure 1) in 1951. These cells were obtained from a tissue biopsy of 30-year-old woman named Henrietta Lacks. In February 1951 she was diagnosed with an aggressive adenocarcinoma of the cervix. Her cervical biopsy supplied tissue to the pathology department at The Johns Hopkins Hospital for a better clinical picture of her state and for future research purposes. At that time, George Gey was trying to isolate and maintain normal and malignant or somehow diseased tissue as temporary or stable cell culture. To grow cells from a tissue in situ, he collected the tissue from surgical procedures from the whole hospital. Despite many previous unsuccessful attempts of stable in situ growth of either normal cervical epithelium or cervical carcinoma in culture, the aggressive adenocarcinoma of Henrietta Lacks gave rise to a first immortal 2D cell culture. Moreover, first published data was in 1952 reporting cases of cervical carcinoma cell cultures (Lucey, Nelson-Rees, and Hutchins, 2009).

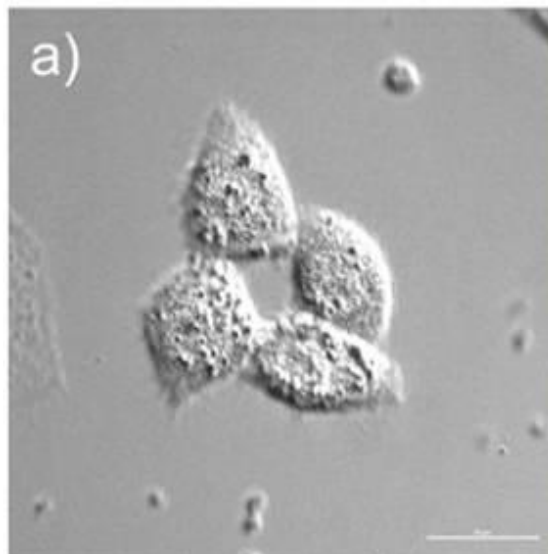


**Figure 1. Brightfield image of HeLa cells.** 2D structure of HeLa cells seen under light microscope (taken from Wang et al., 2017).

### **1.1.2. Normal cell line**

It was in 1975 when James Rheinwald and Howard Green successfully developed first long-term culture of normal non-transformed human cell line. Cells they tried to culture were freshly isolated keratinocytes. However, they have combined them in a dish with previously irradiated 3T3 mouse fibroblasts that were cultured in the same lab, but years earlier. The culture of keratinocytes showed similar behavior as functional human skin. That means that mitosis was limited only to a basal layer of growing clones, whereas the superficial layers contained terminally differentiating keratinocytes that made a cornified cell envelope (Rheinwald and Green, 1975). After some enhancements in the cell culture procedures, scientists were able to cultivate large confluent sheets of epidermis which were grown from relatively small number of primary keratinocytes. But in that time, those cells were still not recognized as stem cells. Nevertheless, Howard Green and his co-workers started to use their cell cultures in medical purposes, too. At the time, they have applied their lab grown sheets of keratinocytes to treat a third – degree burns. For example, in 1980 two patients were given autologous keratinocytes sheets at the Peter Bent Brigham Hospital and successfully recovered afterwards (Clevers, 2016). After a success with keratinocytes, Rheinwald tried to establish a different human cell culture, the cornea cells. Methodology he used was similar to one used to culture keratinocytes, which was then later used to successfully treat patients with cornea blindness (Lindberg et al., 1993).

### **1.1.3. Organoids**

When advanced culture methods first arise, scientific research community was able to culture miniature „organs in a dish“ (Sato and Clevers, 2015). Those advanced methods enabled scientists to mimic in vivo niche of an organism by defining tissue specific growth factors and signaling molecules; and development of cell structures in three dimensions due to a novel culturing methods using different hydrogels which provide stable and firm environment for cells to grow in 3D. Organoids or “organs in a dish” are novel and more physiological than 2D cell cultures model for healthy and cancer tissue. After embedding in 3D matrix or hydrogel organoids can be grown into self-organizing organotypic structures which resemble their native counterparts (Drost and Clevers, 2018). First experiments with organoids were done in 1965 and they were popular to work with up until 1985 which is seen by an increase in PubMed search term „organoids “. At that time, the term was popular in classic developmental biology and was used to describe organogenesis research by cell dissociation and reaggregation. Those experiments were a great start point since they demonstrated enormous self-organizing potential

of vertebrate cells (Lancaster and Knoblich, 2014). However, after the first peak, organoids were not again a subject of intensive research until past 10 – 15 years. The crucial moment was when organoids were defined as 3D structures grown from different types of organ-specific stem cells that self-organize through cell sorting and spatially restricted lineage commitment (Clevers, 2016).

Few requests must be fulfilled to define a collection of cells as an organoid. First, more than one cell type which makes an organ must be present in the culture. Moreover, it should exhibit at least some functions related to its native organ, and last, the cells in the organoid should be organized similarly to the cells in the native organ. Thus, we can define organoids as in situ cellular structures containing several cell types that usually develop from either stem cells or organ progenitors and are capable of self-organizing through cell sorting and spatially restricted lineage commitment (Lancaster and Knoblich, 2014).

There are two native sources of stem cells for an organoid culture. First ones are pluripotent embryonic stem (ES) cells which have their synthetic cousins, induced pluripotent embryonic stem (iPSCs) cells. Together they are called pluripotent stem cells (PSCs). Pluripotent stem cells are those from which all the embryonic structures can arise, but not the extra-embryonic tissue. It means that from PSCs can develop tissue from all three germ layers (endoderm, mesoderm, and ectoderm), but not trophoblast whose main role in embryonic development is to protect and nourish the embryo. Normally, pluripotent stem cells are found in the inner cell mass of an embryo, but novel methods in molecular biology enabled scientist to produce iPSCs from any cell given a specific cocktail of molecules responsible for their pluripotency. Second ones are organ restricted adult stem cells (ASCs). Those cells are considered multipotent as they can give rise to more different cell lines from the same tissue. Both iPSCs and ASCs are characterized by their unlimited potential to divide both in vivo and in vitro (Clevers, 2016).

### **1.2.1. Organoids derived from PSCs**

Although the PSCs are stem cells, scientists have managed to differentiate them to form different tissues due to principles of developmental biology. First, all kinds of different cell types were made from those cells, but then the process was taken a step further. System of PSCs in situ successfully recapitulated whole organogenesis in vitro, forming not only different cells, but making the whole organ from those cells combined. Not only that PSCs differentiated in different cell types, but they assumed spatial patterning and morphogenesis of its native organ. Different types of organoids produced in presented way are shown in figure 2. For PSCs to give a rise to a wide range of organoids, it is important to culture them in different growth medium.

When given diverse signaling molecules and growth factors, cells differentiate in a specific lineage manner, following the patterns known from developmental biology (Clevers, 2016).

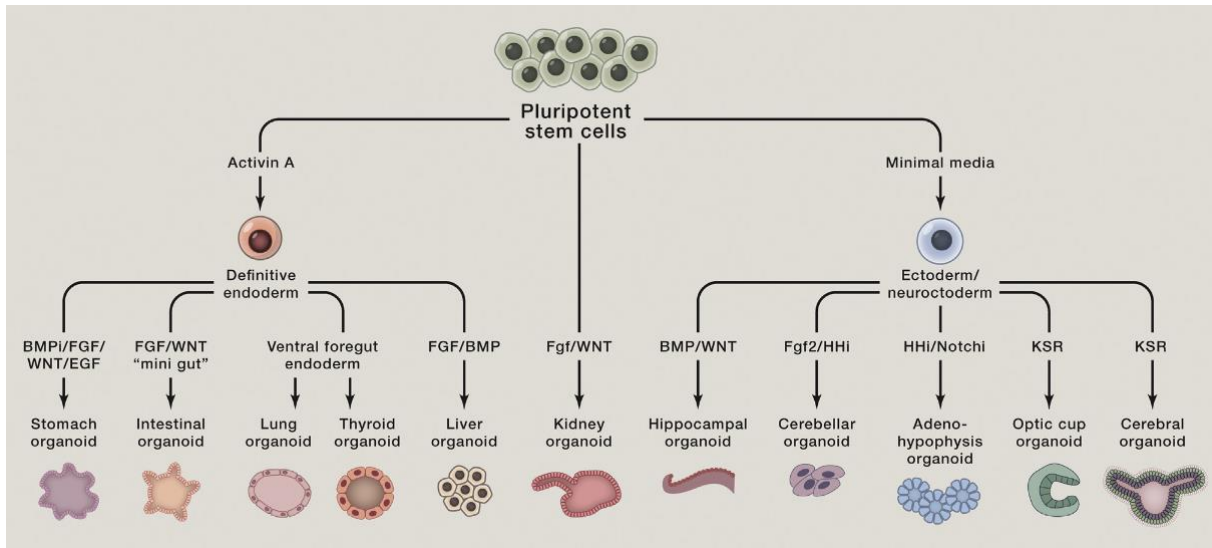


**Figure 2. Different types of organoids that can be made from pluripotent stem cells.** There are eleven different types of organoids that are derived from pluripotent stem cells. Those include stomach, intestinal, lung, thyroid, liver, kidney, hippocampal, cerebellar, adenohypophysis, optic cup, and cerebral organoids. Their differentiation depends on diverse molecules that can be added or excluded from the minimal medium. All the molecules that drive different organogenesis process are listed in the picture (taken from Clevers, 2016).

### 1.2.2. Organoids derived from ASCs

When culturing organoids from adult stem cells, it is crucial to faithfully mimic the conditions of the specific stem cell niche environment present during physiological tissue self-renewal or during damage repair (Clevers, 2016). This principle was initially described for gut stem cells where the Wnt signaling pathway was a primary suspect for driving the stemness of epithelial ASCs. Wnt signaling pathway is one of the most important signaling pathways in humans. The complexity of Wnt signals and their functional role is crucial in both development and growth. Wnt signaling pathway is very important during embryogenesis where Wnt signals facilitate new organism formation by inducing cell differentiation, polarization, and migration. Activation of Wnt signaling pathway is also commonly known to happen during development of many tumors and other serious diseases such as Alzheimer’s disease. The most important component of the Wnt signaling pathway is the family of the Wnt proteins whose main role is activating cell membrane receptors in paracrine and autocrine approach. Secreted Wnt proteins can induce cellular mechanisms of differentiation by activating Frizzled (Fzd) membrane

proteins and by producing transcription factors which regulate gene expression (Taciak et al., 2018). One of the most important Wnt protein is Wnt3A protein which binds to the LRP5/6 receptor in the Wnt signaling pathway and induces gastrulation in an organism by blocking primitive streak and consequently mesoderm and endoderm formation. The receptor for the secreted Wnt-amplifying R-spondins, Lgr5+ (leucine-rich repeat-containing G-protein coupled receptor 5) is a molecular marker of active adult stem cells in epithelia. Lgr5+ encodes a receptor with seven transmembrane domains which belongs to the rhodopsin family of G protein-coupled receptors. Lgr5+ and its closely related homologs Lgr4+ and Lgr6+ are high affinity coreceptors of the secreted growth factors R-spondin 1, 2, 3, and 4, which also bind to the transmembrane E3 ubiquitin ligases Rnf43/Znrf3. In the absence of R-spondin molecules, ubiquitin ligases Rnf43/Znrf3 antagonize Wnt signaling by targeting Fzd receptors for degradation. Binding of R-spondin molecules to the receptors Lgr4+, Lgr5+ or Lgr6+ sequesters Rnf43/Znrf3, resulting in stabilization of the Wnt/Fzd receptor complex at the cell surface and concomitant amplification of canonical b-catenin-dependent Wnt signaling (figure 3).

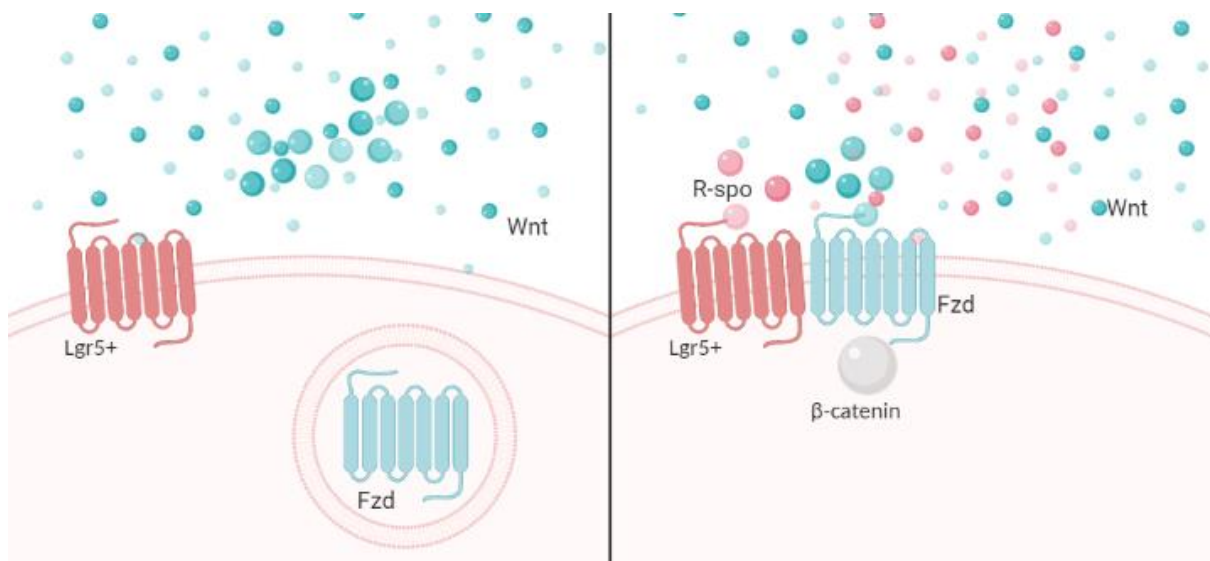


**Figure 3. Wnt signaling pathway depends on the presence of R-spondin molecules.** When R-spondin (R-spo) molecules are not present and Lgr5+ receptor is lacking its substrate, Frizzled (Fzd) receptor gets internalized and cannot bind Wnt molecules (left panel). However, in the presence of R-spondin molecules which bind to Lgr5+ receptor, Fzd receptor is stabilized which allows binding of the Wnt molecules and activation of Wnt signaling pathway including binding of  $\beta$ -catenin protein.



As the *Lgr5+* and *Rnf43/Znrf3* are also transcriptional targets of Wnt/b-catenin signaling, this constitutes an intricate feedback mechanism in which canonical Wnt pathway propagation necessitates the presence of both R-spondin molecules and Wnt ligands (Leung, Tan, and Barker, 2018). Therefore, the key components of most growth media in ASCs culture protocols are Wnt signaling pathway activators, including Wnt3A, R-spondins, and small molecule GSK3 inhibitor CHIR (Clevers, 2016). In the absence of Wnt signaling stimulus, glycogen synthase kinase 3 (GSK3) degrades  $\beta$ -catenin receptor in Wnt pathway which immediately stops stem cell differentiation and proliferation (Krausova and Korinek, 2014).

Organoids derived from adult stem cells are shown in figure 4.

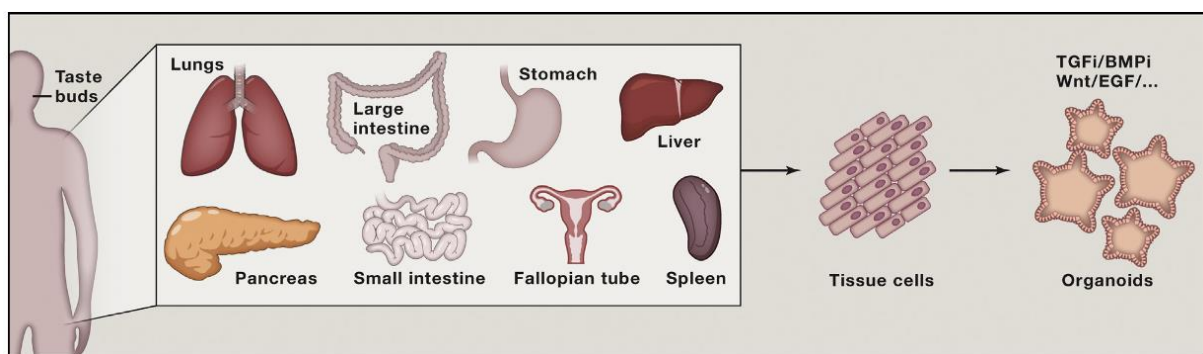


**Figure 4. Types of organoids derived from ASCs.** It is possible to culture lungs, large intestine, stomach, liver, pancreas, small intestine, fallopian tube, spleen, and taste buds organoids from ASCs. It is necessary to isolate tissue cells from the organoids, which when cultured in an appropriate, organ-specific medium give rise to organoids (taken from Clevers, 2016).

### 1.3. Stem cells

Stem cell technologies promise great advances in personal medicine and treatments. They could be used to analyze disease mechanisms and develop potential therapies. However, they are used in research purposes, too, since modeling development of humans or other species is enabled with modern stem cell technologies (Chagastelles and Nardi, 2011).

The main characteristics which define stem cells are their unlimited dividing potential and self-renewal as well as their differentiation potential. It means that stem cells have the potential to differentiate in all the cell types of the organism. This is, however, only true for some types of the stem cells. While totipotent and pluripotent stem cells, which arise only in early embryonic stages of development, indeed have the potential to give rise to all cell types of an organism, more differentiated multipotent and unipotent stem cells slowly lose that capacity. Multipotent

cells are usually tissue specific and can only make cell types of one specific organ where their stem cell niche is located. This means that stem cells in a small intestine can only produce typical cells that reside in adult small intestine, but not neurons or hepatocytes. When it comes to unipotent cells or progenitor cells, they can self-renew, but a property that makes them questionably stem cells is their ability to only produce one cell type. However, they are usually considered as stem cells despite this diversity from the initial definitions (Zakrzewski et al., 2019).

#### 1.4. Small intestine: development, structure, and function

The adult gastrointestinal tract (figure 5) is composed of few connected organs, including esophagus, stomach, small intestine and colon (Wang et al., 2019).

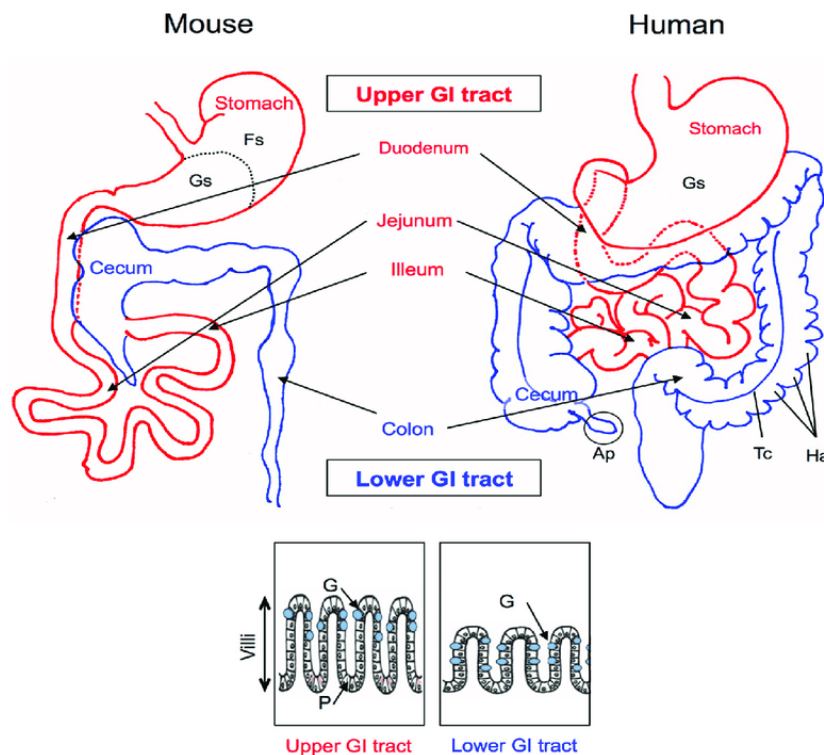


**Figure 5. Mouse and human abdominal anatomy.** The gastrointestinal (GI) tract is divided in two major regions: the upper (red) and the lower (blue) GI tract. The rectangles show schematic models of the villi of the upper and lower gastrointestinal tracts. G represents goblet cells; P represents Paneth cells; Fs represents forestomach; Gs represents glandular stomach; Ap represents appendix; Tc represents taenia coli; Ha represents haustra (taken from Keita, Makoto, and Takao, 2016).

The intestine can be anatomically and functionally divided in the small intestine and the large intestine. The large intestine consists of the cecum, appendix and colon which comprises the

ascending colon, transverse colon, descending colon, and sigmoid colon. The small intestine is composed of the duodenum, jejunum, and ileum (Zietek and Rath, 2018). Histologically, there two compartments of the small intestine could be discriminated, villi, and crypts (figure 6).

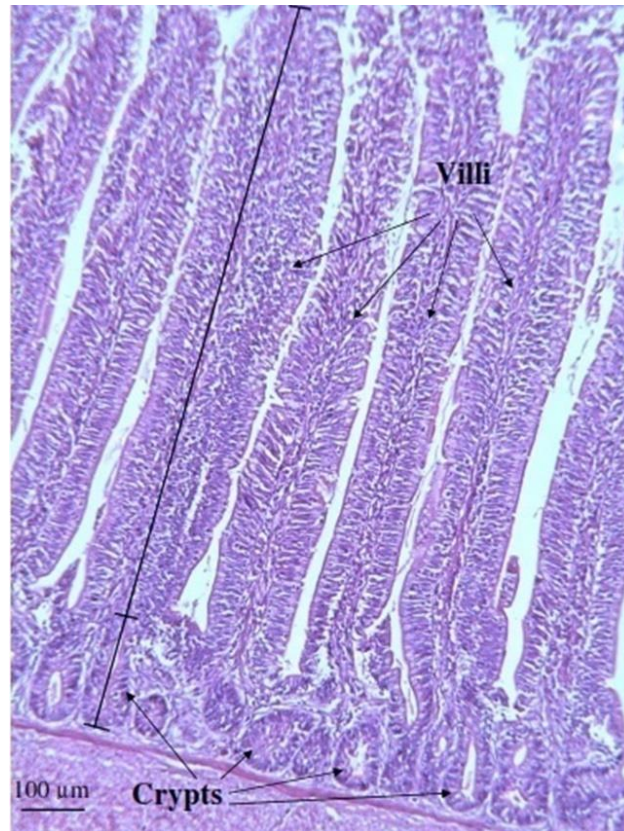


**Figure 6. Histological view of the small intestine.** A cross-section of the small intestine histology shows two major elements: long villi and inner-positioned crypts (taken from Shokryazdan et al., 2017).

Villi are finger-like protrusions pointing toward the lumen, whereas crypts are invaginations into the submucosa (Sato and Clevers, 2012). The main purpose of the intestine is the absorption of nutrients from ingested food. Therefore, the most abundant cell type in the intestine is enterocytes. Their role is to absorb water and nutrients which is done by specific nutrient transporters in their brush border membrane (Daniel and Zietek, 2015). Most nutrient transporters are localized in duodenum and jejunum since the most nutrient and mineral uptake after food ingestion happens there (Yoshikawa et al., 2011). Another part of the small intestine, ileum, is the place where aggregations of gut associated lymphoid tissue (GALT) localizes. They have an important role making gut an immune organ. The large intestine is, however, responsible for fluids intake. Besides the absorption role of enterocytes, goblet cells secrete mucus, enteroendocrine cells secrete intestinal hormones and Paneth cells secrete antibacterial

substances (Sato and Clevers, 2012). Recently, between Paneth cells another type of crypt base columnar (CBC) cell was discovered, expressing *Lgr5* and possessing stem cell properties which include multipotential differentiation and long-term self-renewal (figure 7). These CBC and Paneth cells are found at the base of the crypt, while other cell types, including enterocytes, goblet cells and enteroendocrine cells move towards the peak of the villi (van Barker et al., 2007).

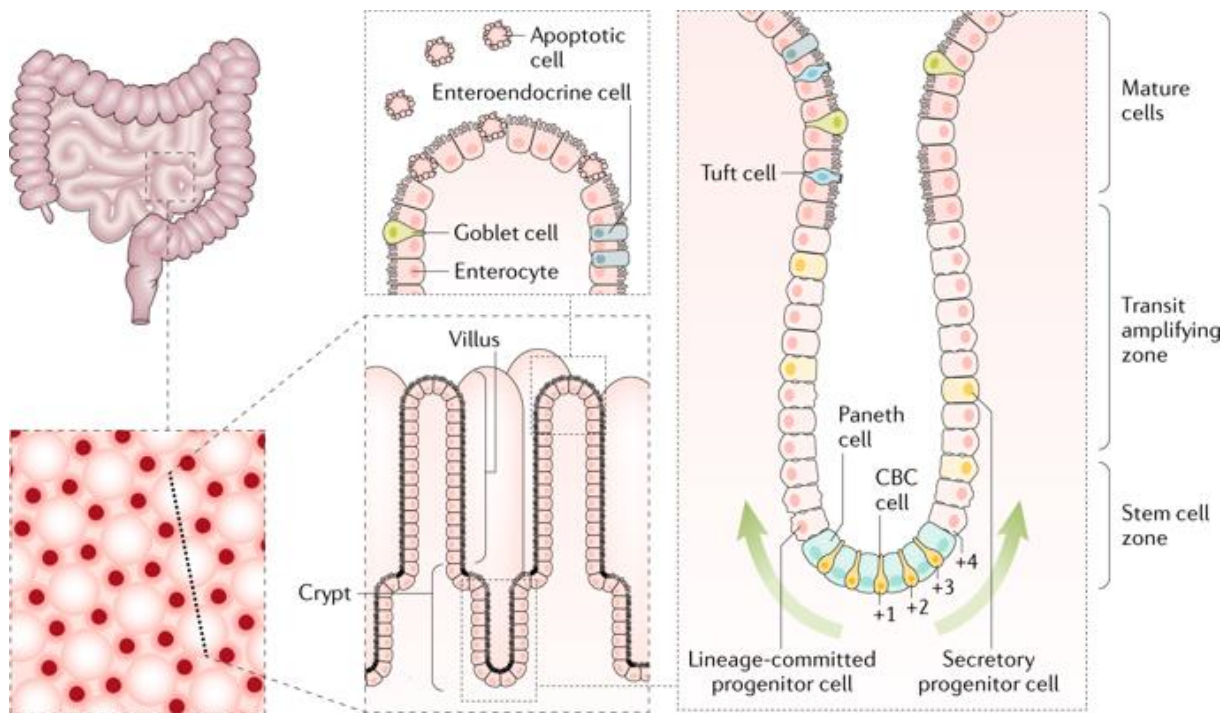


**Figure 7. The location and structure of crypts and villi.** Crypts are divided into three zones: stem cell zone containing Paneth and CBC cells; transit amplifying zone and mature cells zone. The villi contain fully differentiated cells including enterocytes, Goblet cells and enteroendocrine cells (EEC). There are apoptotic cells floating surrounding the villi (taken from Gehart and Clevers, 2017).

Most parts of the gastrointestinal tract derive from the embryonic endoderm germ layer. Foregut forms the proximal part of the duodenum, up to the entrance of the bile duct, whereas the midgut forms a big part of alimentary canal, from the bile duct to the proximal parts of the transverse colon. Lastly, the hindgut forms the distal parts of the colon including the transverse colon, the descending colon, sigmoid colon, and rectum. The function of intestine is under regulation of enteric nervous system (Gehart and Clevers, 2017).

The gastrointestinal tract is composed of four layers which surround it: the mucosa, the submucosa, the muscularis layer and the serosa or adventitia. The external layer is serosa. It is

formed by connective tissue and it encloses the muscle layers and the myenteric plexus of the muscularis layer. The submucosa makes a connection between the inner mucosa and outer muscle layer and supports their function. The submucosa is also formed by connective tissue including nerves, large blood vessels and lymphatics. The mucosa is the inner layer of the gastrointestinal wall and is divided in three parts. The first, muscularis mucosae represents a thin layer of smooth muscle, followed by the lamina propria, a layer of connective tissue which contains a large number of immune cells (figure 8). Finally, the epithelium is a monolayer of intestinal epithelial cells (IECs) which cover the intestine and make a barrier between lumen and the host. IECs are responsible for most of the digestive, absorptive and secretory functions of the intestine (Zietek and Rath, 2018).

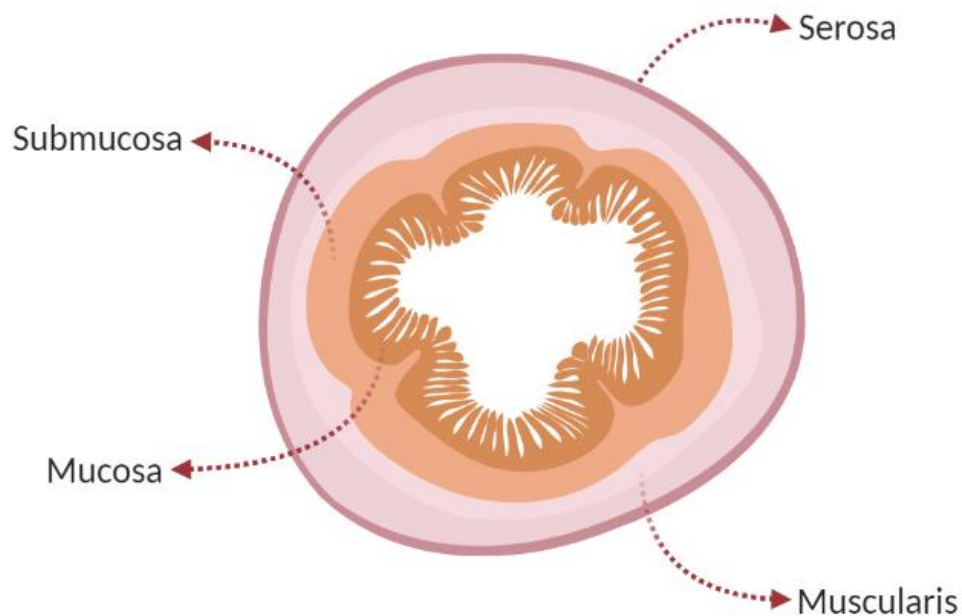


**Figure 8. Composition of the gastrointestinal tract.** Mouse gastrointestinal tract is built up from four layers starting from the outer most: serosa, muscularis, submucosa and mucosa.

The intestine morphology is not unique throughout its length. For example, while small intestine is histologically built from crypts and villi structures, the large intestine does not contain them. Moreover, the length of the villus increases from duodenum to ileum, making ileum the part of small intestine with the longest villi (Zietek and Rath, 2018).

### 1.5. The need for small intestine organoids

For a long time, a unique and satisfactory in vitro model of intestinal epithelium has not been available. For that reason, for a long-time no model could satisfactorily mimic the diversity nor complexity of the small intestine. Moreover, since primary cultures of intestinal epithelial cells

rapidly enter apoptosis, their cultivation is still not successfully developed for longer timeframes. Another problem is the diversity of cells within the small intestine. Not all cell types are equally successfully cultivated. Therefore, the information obtained from the primary cell cultures of the small intestine is limited and the complexity of the organ may be underappreciated. There are some problems with secondary intestinal epithelial cell lines, too. They are mostly genetically modified in some manner or originate from tumor tissue which makes them physiologically different from natural intestinal epithelial cells. Furthermore, most immortal intestinal cell lines are restricted to only one cell type of IECs which limits any studies of complex intercellular interactions between IECs cells (Zietek and Rath, 2018).

On the other hand, recently established small intestine organoids can be kept in culture for longer periods of time. They well represent the complexity of cell types and interactions present within natural intestine, since they usually contain all different IECs, including adult stem cells, mucin-producing goblet cells, antimicrobial peptide-producing Paneth cells, tuft cells, hormone-producing EEC and absorptive enterocytes. Also, an important feature of organoids is their location-specific function and gene expression throughout long-term culturing (Sato et al., 2009).

Small intestine organoids are mostly made for three purposes: (1) to model organ development and morphogenesis; (2) to model different intestinal diseases; and (3) for usage in regenerative or personalized medicine (Clevers, 2016).

### **1.6. Growth factors and signaling**

Small intestine organoids or enteroids are initially grown from small intestine crypts containing adult intestinal stem cells. Marker of those cells is *Lgr5*<sup>+</sup>. Harvested crypts are induced to differentiate and self-renew by addition of EGF (epithelial growth factor), R-spondin and Noggin. Growth factor EGF is needed when culturing small intestine organoids for long term culture because it induces epithelial cell survival. R-spondin is mostly expressed by subepithelial fibroblasts. It binds to the *Lgr5*<sup>+</sup> receptor and suppresses the degradation of Wnt receptors on the stem cells. This prevented degradation of Wnt receptors allows Wnt activation which is important for maintenance of cell stemness. Paneth cells produce several different Wnt ligands and therefore assure the production of Wnt which is essential to maintain adult intestinal stem cells in the native intestine (Wallach and Bayrer, 2017). Similarly, small intestine organoids constitutively express Wnt reporters at their budding structures, due to Paneth cells in the bottom of the crypts. The central role of Wnt signaling is the maintenance of undifferentiated crypt progenitor state. Hence, the addition of Wnt3A to small intestine

organoids culture interferes with differentiation of organoids and yields undifferentiated, cystic organoids which consist mostly of progenitor cells. Wnt3a is usually added to small intestine organoids 2 days after crypt isolation to help Paneth cells reestablish normal, physiological Wnt pathway signaling levels (Sato et al., 2011). Another component, Noggin, a secreted glycoprotein, works as BMP antagonist. BMP signaling pathway is involved in epithelial differentiation and negatively regulates the number of stem cells (figure 9). The BMP signaling pathway is strongly activated in differentiated cells, as demonstrated by the expression of phosphorylated SMAD1, SMAD5, and SMAD8, downstream molecules of BMP signaling (Date and Sato, 2015). It was proven that Noggin is essential for long-term maintenance of small intestine organoids cultures. When organoid small intestine cultures were deprived of Noggin, organoids lost *Lgr5*<sup>+</sup> expression and their proliferation stopped after 2 weeks in culture. BMP is a mesenchymal product probably responsible for differentiation of small intestine organoids. His role is also described in pathways maintaining adult stem cells (Wallach and Bayrer, 2017).

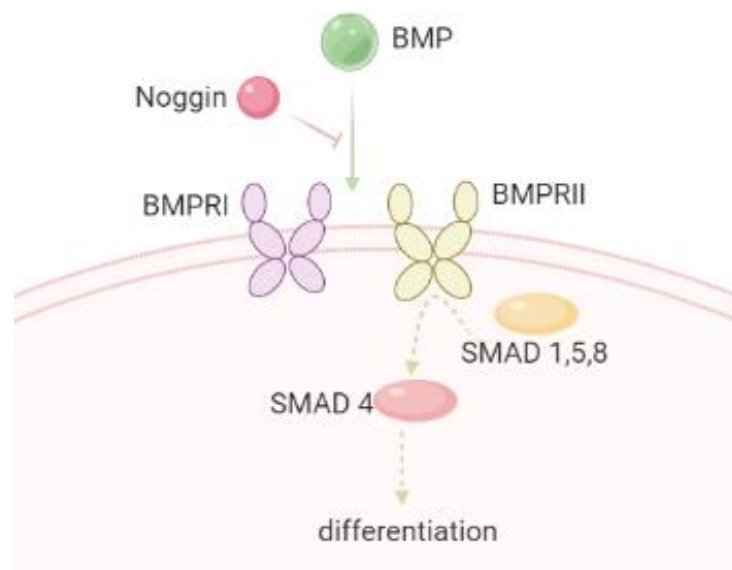


**Figure 9. Noggin is the antagonist of BMP signaling pathway.** Noggin protein works as inhibitor of BMP signaling pathway by preventing BMP molecule from binding to BMP receptors (BMPRI and BMPRII) which causes their dimerization and phosphorylation of SMAD 1, 5, and 8 molecules. SMAD 1, 5, and 8 then activate SMAD 4 which activates cellular differentiation.

The base medium in which all the growth factors are added is usually DMEM F12/Advanced medium. The color of the medium is light red due to presence of phenol red indicator. When at physiological pH (7,0-7,4) the described light red color appears. However, if the pH changes to acid, color of the medium changes to yellow. On the other hand, if for some reason the medium becomes basic, it will change color to purple.

### **1.7. Therapeutic potential of the organoids**

Besides modeling basic scientific principles, the other obvious advantage of culturing organoids is disease modeling and therefore, it will probably be the focus of future organoid studies. The spectrum of diseases requiring more complex modeling is very broad, from cancer, degeneration, infectious disease to developmental disorders. It is conceived that patient derived organoids will also have an important role in future disease modeling and drugs validation (Lancaster and Knoblich, 2014). For example, kidney organoids were recently generated from patients-derived induced pluripotent stem cells, although differentiation of pluripotent cells into renal lineages has not shown much success earlier. Therefore, this organoid model should be an important step towards understanding kidney disorders (Xia et al., 2013). Another way to use organoids is to make them from healthy, normal cells, but use modern genome-technologies to introduce different mutations which are known to induce severe disorders. Also, brain organoids are a very useful model for various neurodevelopmental disorders. They have been used first to model and explain microcephaly, but have potential to explain more complex disorders such as autism, epilepsy, or schizophrenia (Lancaster et al., 2013).

Another potential of organoids is testing efficacy and toxicity of drug compounds. In this manner organoids could be used for drug screening experiments thereby decreasing the use of animal testing. Organoid approach also brings a few advances regarding the specific organs, like liver, whose metabolism significantly differs between humans and model animals. Using organoid approach, all the experimental results done on the liver cells would immediately be more relevant and trustworthy (Clevers, 2016).

A big advantage of organoids in clinic is the possibility to replace current cell or whole organ replacements strategies. Organoids isolated from patients' tissue could potentially provide a good source of autologous tissue for transplantation. However, the biggest disadvantage of organoids for usage in whole transplantation procedures is their lack of vascularization. Because of those limitations, it is currently challenging to supply all the cells in a big organ with their daily requests for nutrients and oxygen. The biggest organ yet developed in situ for



transplantation is a mouse kidney. Any bigger organ is predicted to not succeed in its needs for food and oxygen after transplantation procedure (Lancaster and Knoblich, 2014).

Summary of all the scientific and medical possibilities of organoids usage is given in figure 10.

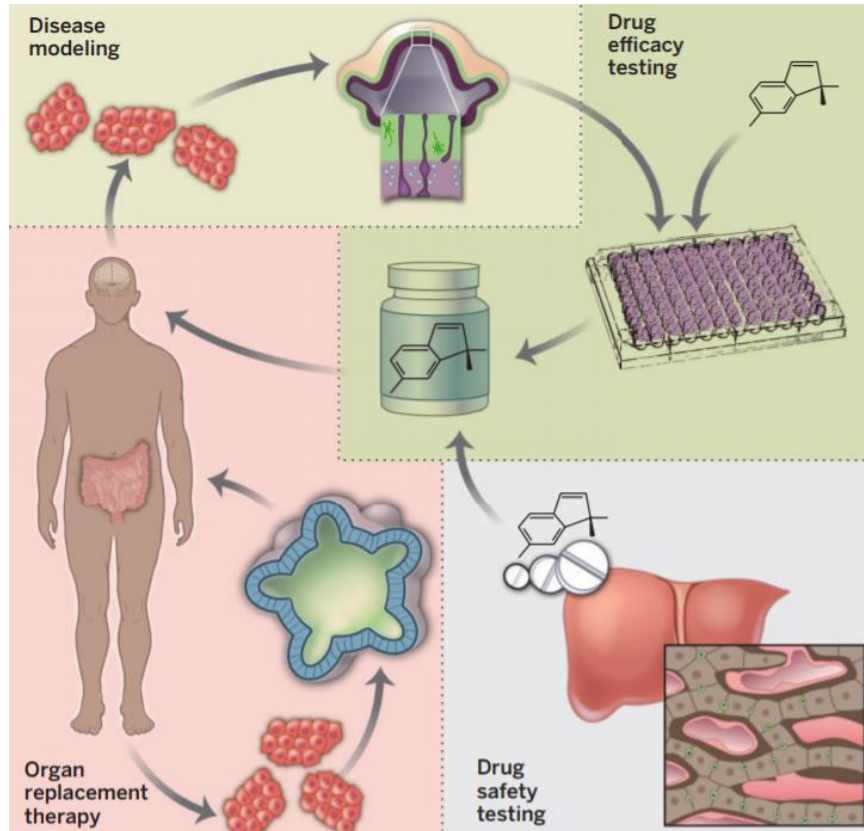


**Figure 10. Potential uses of organoids.** Organoids can be used to model different diseases, to test drug efficacy and safety, without the need for laboratory animals and also as a potential organ replacement therapy (taken from Lancaster and Knoblich, 2014).

### 1.8. The research aims

The main aim of this research was to successfully establish a culture of mouse small intestine organoids. The goal was to optimize the protocols of mouse small intestine isolation, mechanical dissociation, and crypt seeding. To estimate the efficiency of the protocols, mouse small intestine organoids were immunolabeled and bioimaged using confocal microscopy. The purpose of bioimaging the organoids was to precisely define their morphology and proliferation status. Therefore, DNA and actin stains and  $\alpha$ -tubulin antibodies were used to obtain the information about the morphology of developed mouse small intestine organoids, whereas Ki-67 antibody was used to determine their proliferation rate.

## **Materials and methods**

### **2.1. Thawing of cryovial with small intestine organoids**

Cryovials with small intestine organoids were a gift from prof. Geert Kops, Hubrecht Institute, Utrecht, Netherlands.

Cryovials are stored in liquid nitrogen prior to usage. Small intestine organoids are thawed quickly in 37 °C water bath (approximately 1 min or until almost all content is liquid). Organoids are collected with a pipet into a 15 mL conical tube. Organoid basal medium (OBM, composition detailed bellow) is added (12 mL) to the tube and the tube is gently inverted. Organoids are spun down in a centrifuge (500 g, 5 min, RT). Washing step and centrifuge is repeated (remove 8 mL of OBM and add new 8 mL of OBM). The supernatant is removed and discarded. Organoids are suspended with 50 µL of Matrigel. Matrigel with organoids is dispersed on a prewarmed 24-well plate in a small drop of 15 µL. The plate is incubated 10 min at 37 °C, 5% CO<sub>2</sub>. Intestinal culture medium (ICM) is added (500 µL) per well.

The viability of the organoids was suspected by the color of the medium in the cryovial where red color suggested normal, physiological state of the organoids and yellow color proposed that something is wrong with the organoids which caused the change in the pH of the medium.

### **2.2. Mouse small intestine isolation**

Mice (figure 11 and 12) were sacrificed according to applicable ethical regulations. Abdomen of the mouse was wet with 70% ethanol. The abdominal cavity was cut open by carefully cutting the skin and fur and then cutting the thin membrane protecting the internal organs (figure 13). The position of gastrointestinal tract was determined (figure 14). First, the stomach was found and then it was pulled out along with the intestines. Next, sacum was localized and small intestine was cut between stomach and sacum. This part was done by Iva Bazina from Laboratory for Neurodegenerative disease research, Ruđer Bošković Institute, due to formal regulations that define work with live laboratory animals.

Isolated small intestine was placed in cold PBS (phosphate buffer solution). Adjacent tissue, including blood vessels, fat and connective tissue was removed using forceps.

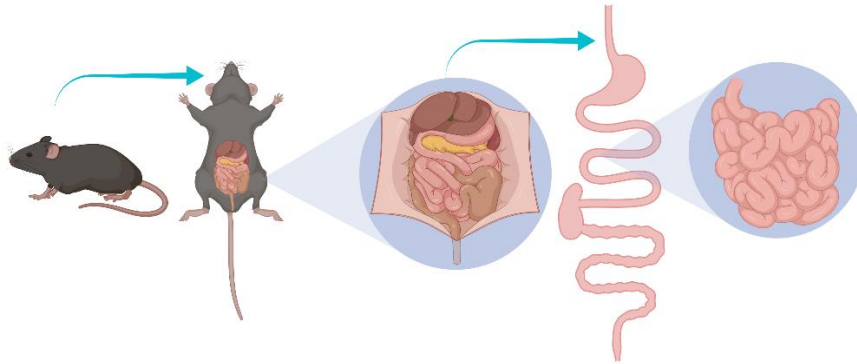


**Figure 11. The anatomy of mouse internal organs.** The goal of isolation is to localize and carefully take out the small intestine, without any damage to the organ.

The impurities inside the small intestine were first extruded using mechanical force by fingers. They were then flushed by injecting cold PBS inside the small intestine using a thin syringe. Small intestine was then cut in four pieces (approximately 5-7 cm long) and cut open with scissors so that the luminal side was facing upwards (figure 15, A). Afterwards, intestine was then cleaned more by scratching lumen of the small intestine with glass microscope slide (figure 15, B) until the intestine was pale pink color. Summary is given in figure 16.

A)



B)



**Figure 12. Sacrificed mouse.** A mouse (A) was sacrificed in concordance with ethical regulations and outspread to ease the dissection (B).



**Figure 13. Dissection of the mouse.** After cut opening the skin and the fur, a thin layer of membrane protecting the organs must also be cut and removed.



**Figure 14. Mouse prepared for isolation of the small intestine.** After removing all the barriers, mouse gastrointestinal tract (yellow circle) can be isolated.

A)



B)

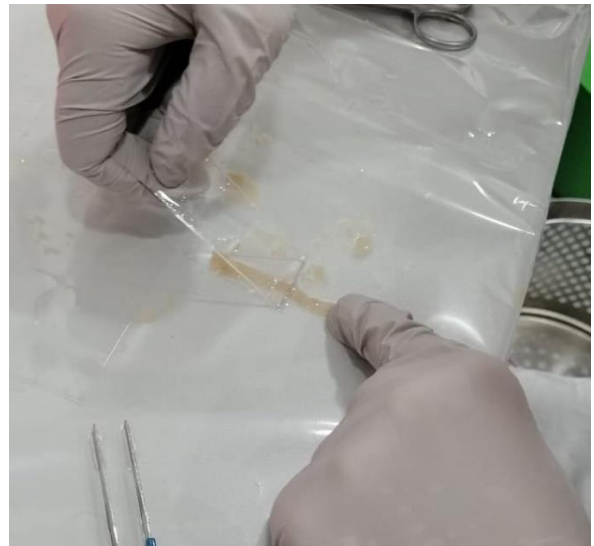


**Figure 15. Process of mouse small intestine dissection and crypts isolation.** A) Opening a part of the mouse small intestine. B) Scratching all the impurities on the inner side of the small intestine with glass slide.

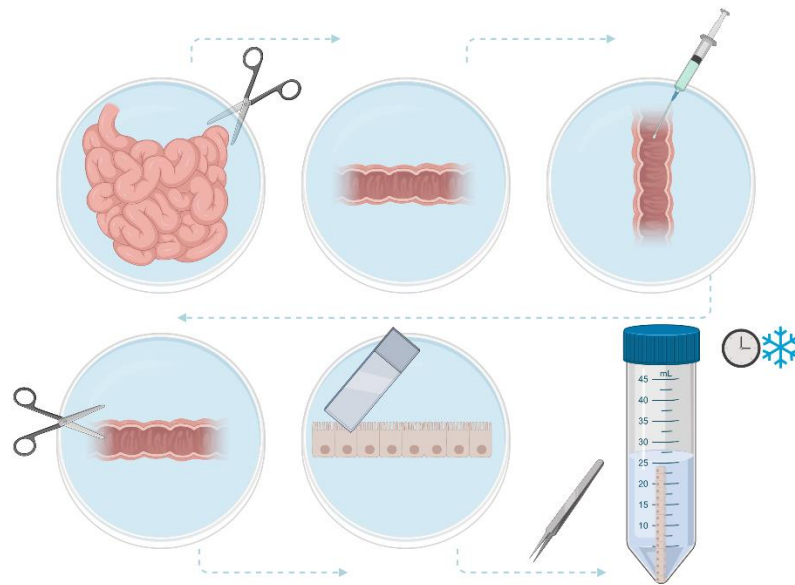


**Figure 16. Schematic representation of cleaning the impurities from mouse small intestine.** After carefully dissecting the small intestine, it is cleaned mechanically by pushing any residing objects out of the intestine. Then, the intestine must be washed out with cold PBS and afterward cut to open it, but being careful about maintaining the orientation. The inside of the small intestine is then scraped off with a glass slide and incubated in cold 5 mM EDTA/PBS for 30 minutes on ice.

### 2.3. Isolation of the intestinal crypts

All parts of small intestine were transferred into a 50 mL conical tube filled with ice-cold 5 mM EDTA/PBS solution. It was incubated for 30 minutes on ice and flicked every 10 minutes.

Segments of small intestine were transferred into a new 50 mL conical tube filled with 25 mL PBS. The tube was vigorously shaken 10 times and then immediately placed on ice. Parts of the small intestine were transferred back to the tube filled with 5 mM EDTA/PBS.

A fraction (50  $\mu$ L) of the EDTA tube was transferred on microscope slide and was inspected under the microscope (10x objective/40x magnification) to identify the presence of the intestinal crypts (figure 17). The crypts were recognized as thin U-shapes (figure 18) under the microscope which have small cells surrounding a tight gap between the two layers.

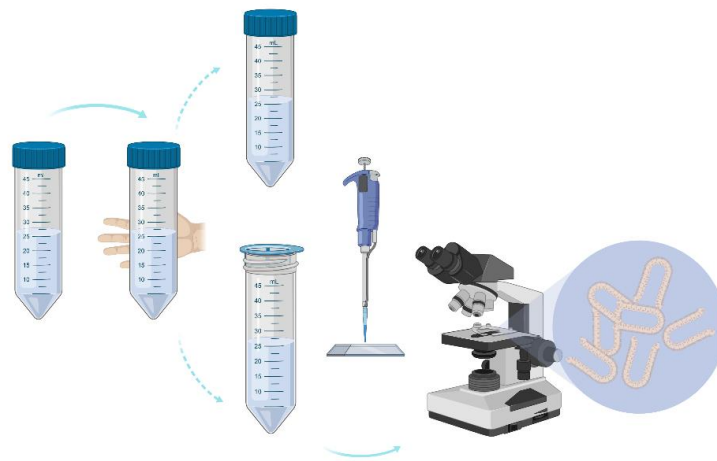


**Figure 17. Schematic representation of crypt isolation.** Post 30 minutes incubation of small intestine in 5 mM EDTA/PBS, the parts of the intestine are transferred to a tube with PBS. The tube is well shaken 10 times and then the parts of the small intestine are transferred back to 5 mM EDTA/PBS tube. The tube containing EDTA is filtered and a small drop is inspected for the presence of crypts under the microscope.



**Figure 18. Crypts isolated from mouse small intestine.** After a successful crypt isolation, they are seen as thin U-structures (red circles) under the microscope. Scale bar is 20  $\mu\text{m}$ .

## 2.4. Seeding small intestine crypts

Small intestine crypts are span down in a centrifuge (500 g, 5 min, RT). Half of the supernatant is removed. Other half is transferred to a new 15 mL conical tube. Equal amount of organoid basal medium (OBM, table 1) is added. The tube is again span down in a centrifuge (500 g, 5 min, RT). Supernatant is completely removed. Desired amount of Matrigel is added (25  $\mu$ L/100 – 200 crypts). The pellet was carefully pipetted up and down 10 times to thoroughly resuspend the pellet. Everything was kept on ice.

**Table 1. The composition of organoid basal medium (OBM).** Expect for Advanced DMEM/F12, the medium contains Glu – Ala supplement, Penicillin/Strep and HEPES buffer.

OBM	Stock	Dilution	Final concentration	For 500 mL
Advanced DMEM/F12				444,8 mL
Glu - Ala	200 mM	1:1000	0,2 mM	200 $\mu$ L
Penicillin/Strep	100%	1:100	1%	5 mL
HEPES	10 mM	1:10	1 mM	50 mL

Few small drops (14  $\mu$ L) of Matrigel suspension are applied per well on the 24 hours prewarmed 24-well plate. The suspension is added far from the edges of the well to form a hemispherical droplet (figure 19).

The plate is incubated at 37 °C/ 5% CO<sub>2</sub> to solidify for approximately 5 – 10 minutes (figure 15). The Matrigel droplet is finally covered with 500  $\mu$ L of crypt culture medium (CCM) (table 2).

**Table 2. The composition of crypt culture medium (CCM).** The base for CCM is made of OBM explained in Table 1 and supplemented with B27, N-Acetylcystein, mEGF, Noggin, R-spondin 1, Wnt3A and Y-27632.

CCM	Stock	Dilution	Final concentration	For 10 mL
OBM				9,61 mL
B27 supplement	50x	1:50	1x	200 $\mu$ L
N-Acetylcystein	500 mM	1:500	1 mM	20 $\mu$ L
mEGF	20 $\mu$ g/mL	1:400	50 ng/mL	25 $\mu$ L
Noggin	50 $\mu$ g/mL	1:500	100 ng/mL	20 $\mu$ L
R-spondin 1	50 $\mu$ g/mL	1:100	500 ng/mL	100 $\mu$ L
Wnt3A	50 $\mu$ g/mL	1:500	100 ng/mL	20 $\mu$ L
Y-27632	10 mM	1:4000	2,5 $\mu$ M	10 $\mu$ L



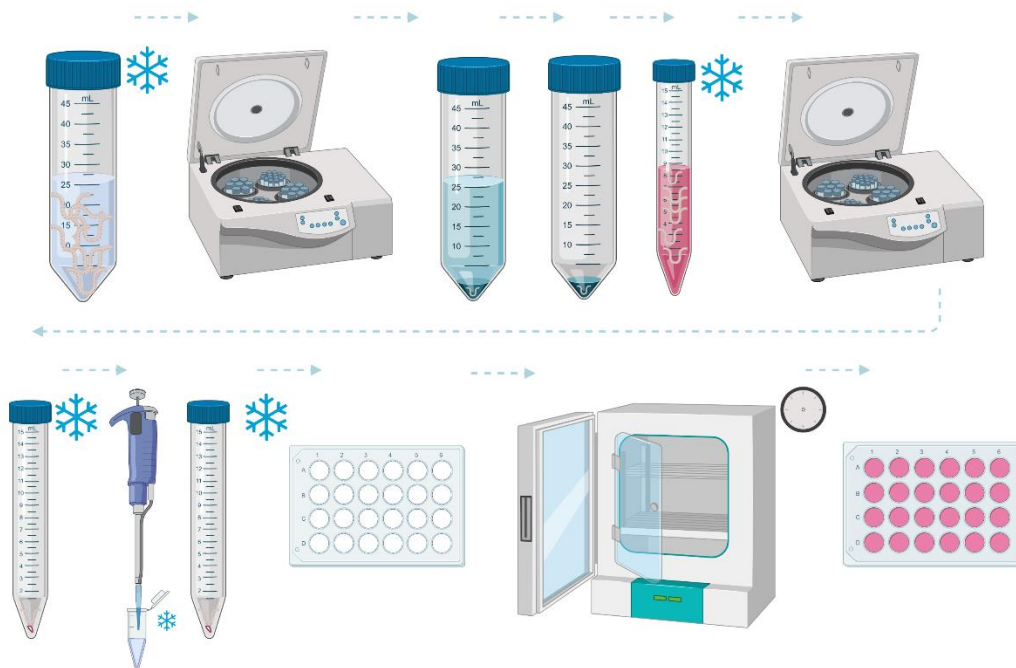


**Figure 19. Schematic representation of culturing isolated small intestine crypts.** When the presence of crypts is confirmed under the microscope, they are spun down, resuspended in OBM, and spun down again. The crypts are then dissolved in Matrigel and seeded on a preheated 24-well plate. CCM is added to the wells after solidification, for 10 minutes incubation on 37 °C and 5% CO<sub>2</sub>.

The medium is changed every two days. First two days after isolation, intestinal culture medium (table 3) is being used.

**Table 3. The composition of intestinal culture medium.** The organoid basal medium (OBM) explained in Table 1 is supplemented with B27, N-Acetylcystein, mEGF, Noggin and R-spondin 1.

ICM	Stock	Dilution	Final concentration	For 10 mL
OBM				9,65 mL
B27 supplement	50x	1:50	1x	200 µL
N-Acetylcystein	500 mM	1:500	1 mM	20 µL
mEGF	20 µg/mL	1:400	50 ng/mL	25 µL
Noggin	50 µg/mL	1:500	100 ng/mL	20 µL
R-spondin 1	50 µg/mL	1:100	500 ng/mL	100 µL

## 2.5. Small intestine organoids splitting

When crypts have reached expected density and size, it is time to split them. Organoids should not be bigger than 250  $\mu\text{m}$  in length or width. Moreover, the cell density should be low enough for the organoid to be transparent. The efficiency of splitting is lower when organoids become dark, grey, or black.

ICM is removed from wells and 800  $\mu\text{L}$  of OBM is added. The well is scratched thoroughly with a pipette tip, so that all the Matrigel droplets are detached. The suspension is transferred to 15 mL conical tube and is spun down in a centrifuge (500 g, 5 min, RT). Supernatant is removed. The pellet is carefully resuspended in Matrigel (25  $\mu\text{L}/100 - 200$  crypts) and small drops (14  $\mu\text{L}$ ) of suspension are seeded on a 24 h prewarmed plate (figure 20).

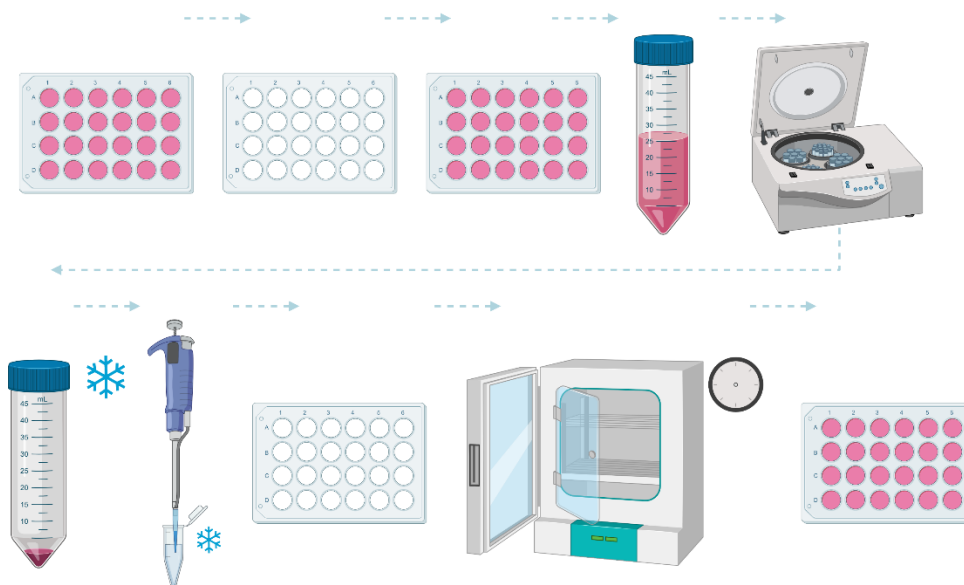


**Figure 20. Schematic representation of propagation of small intestine organoids.** The intestinal culture medium is removed from the wells and organoids basal medium (OBM) is added. The bottom of the well is scratched so that no Matrigel is left behind and the OBM is then transferred to a conical tube. The content is well resuspended 10 times and spun down. The pellet is dissolved in Matrigel, incubated on 37 ° and 5 % CO<sub>2</sub> for 10 minutes and then new ICM is added.

## 2.6. Seeding small intestine organoids for immunolabeling

Matrigel is dissolved in OBM (0,8 mg/mL). Coverslips (12 mm) are cleaned in 96% ethanol, they are let to dry and are positioned in the middle of a well of the 24-well plate. The 24-well

plate is put 24h before the experiment in the incubator on 37 °C to preheat it. Matrigel dissolved in OBM (200 µL) is added to each well. The plate with Matrigel/OBM is incubated on 37 °C for 2h before seeding organoids. Organoids are splitted 1,5 h after dissolving Matrigel in OBM as explained earlier. Instead of resuspending the pellet in Matrigel, it is resuspended in ICM without Wnt3A to the density of 300000 organoids per 500 µL. Prepared suspension (500 µL) is plated in wells with Matrigel dissolved in OBM on preheated 24-well plate. The medium is changed after two days to ICM.

## **2.7. Fixation and blocking**

Immunofluorescence staining protocol is started third day after seeding organoids. Coverslips are transferred to the new clean wells on a 24-well plate. Paraformaldehyde (4%, 500 µL) is added to each well and the plate is incubated 5 min at room temperature. Each well is washed 2x with PBS (500 µL), each wash for 5 min. The sample is permeabilized in 500 µL 0,5% Triton X-100 in PBS for 15 min. The sample is washed 2x with PBS (500 µL), each wash for 5 min. If the immunolabeling of samples with antibodies is not done, the protocol should proceed to staining with DAPI and Phalloidin (see below). Blocking solution (3% BSA/PBS) is added to the sample for 1 hour at room temperature (500 µL).

## **2.8. Immunolabeling**

Humid chamber is prepared for antibody incubation. The sample is incubated with primary antibody (diluted in 3% BSA/PBS) over night at 4 °C. A drop of antibody (50 µL) is added to parafilm and coverslips were incubated upside-down on the drop of diluted antibody on parafilm in a humidified chamber. Coverslips are put back to wells again. The sample is washed 2x with blocking solution (500 µL), each wash for 5 min. Secondary antibody (diluted in 3% BSA/PBS) is added to the sample for 1 hour at room temperature. Coverslips are again incubated upside-down on the drop of diluted antibody on parafilm in humidified chamber. Coverslips are put back to wells again. The sample is washed 2x with blocking solution, each wash for 5 min. All antibodies used in the experiment are listed in table 4.

The Ki-67 protein is a marker for proliferation in cells. It is present in cells during all phases of cell cycle including G1, S, G2 phase and mitosis. However, it is absent in resting G0 phase of the cell cycle. An increase in Ki-67 mark happens during progression through S phase of the cell cycle and remains until end of mitosis. During interphase Ki-67 is found throughout the nucleus, whereas during mitosis it is mostly bound to the chromosomes (Scholzen and Gerdes, 2000).

The antibody for  $\alpha$ -tubulin is bound to  $\alpha$  subunits of  $\alpha\beta$ -tubulin dimer. Tubulin dimers make microtubules, cytoskeleton proteins important in cell division. Microtubules are main components of mitotic spindle, multiprotein complex which segregates chromosomes in two daughter cells (Wloga, Joachimiak, and Fabczak, 2017).

**Table 4. Antibodies used in the experiments.** Different primary and secondary antibodies for  $\alpha$ -tubulin and Ki-67 were used.

Protein of interest	Antibody		Producer	Dilution
$\alpha$ -tubulin	Primary antibody	Rabbit T3526	Sigma-Aldrich (Merck-KGaA), St. Louis, MO, SAD	1:100
	Secondary antibody	Alexa Fluor 594-conjugated donkey anti-rabbit antibody	AbCam, Cambridge, UK	1:500
		Aberrior StarRed anti-rabbit KK114 antibody	Aberrior GmbH, Gottingen, GER	1:500
Ki-67	Primary antibody	Rabbit Anti-Ki67 antibody	AbCam, Cambridge, UK	1:100
	Secondary antibody	Aberrior StarRed anti-rabbit KK114 antibody	Aberrior GmbH, Gottingen, GER	1:500
		Aberrior StarOrange anti-rabbit KK114 antibody	Aberrior GmbH, Gottingen, GER	1:500

## 2.9. DAPI and Phalloidin staining

Coverslips are incubated with phalloidin (1:200 in PBS) and DAPI (1:1000 in PBS) for 30 min at room temperature. The sample is washed 2x with PBS, each wash 5 min. Coverslips are dried in 96% ethanol, excess ethanol is tipped off and air dried. Coverslips are mounted onto microscope slide where 5  $\mu$ L of liquid mounting medium is previously added. The sample is left to dry overnight on room temperature and next day is sealed with nail polish for long term storage.

## **2.10. Microscopy**

Bright-field imaging was done on Carl Zeiss Opton inverted microscope with powers supply invertoscope under magnifications of 61x and 160x.

Immunocytochemistry imaging of unlabeled small intestine organoids was performed on two microscopes. First was Bruker Opterra Multipoint Scanning Confocal Microscope (Bruker Nano Surfaces, Middleton, WI, USA). The system was mounted on a Nikon Ti-E inverted microscope equipped with a Nikon CFI Plan Apo VC 60x/1.4 numerical aperture oil objective (Nikon, Tokyo, Japan). To obtain the optimal balance between spatial resolution and signal-to-noise ratio, 22- $\mu$ m slit aperture was used. Opterra Dichroic and Barrier Filter Set 405/488/561/640 was used to separate the excitation light from the emitted fluorescence. Following emission filters were used: BL HC 525/30, BL HC 600/37, and BL HC 673/11 (all from Semrock, Rochester, NY, USA). Images were captured with an Evolve 512 Delta Electron Multiplying Charge Coupled Device (EMCCD) Camera (Photometrics, Tucson, AZ, USA) using a 150 ms exposure time. Electron multiplying gain was set on 500. Camera readout mode was 20 MHz. No binning was performed. The xy-pixel size in the image was 83 nm. The system was controlled with the Prairie View Imaging Software (Bruker).

Other images were taken on Andor Dragonfly multi-point confocal microscope (Andor, Oxford Instruments, UK) for high-speed and high-sensitivity imaging. The system was mounted on Nikon Ti2 inverted microscope (single deck) equipped with CFI P-Apo 63x Lambda / NA 1.40 / WD 0.13 mm – oil (MRD01605) objective (Nikon, Tokyo, Japan). Following emission filters were used: 445/46, 521/38, 594/43, 620/60, 685/47 and 478/37. Images were captured with 1x Andor iZyla EMCCD camera (Andor, Oxford instruments, UK) using 100 ms exposure time. No binning was performed. The xy-pixel size in the image was 100 nm. The system was controlled with the Imaris Fusion Imaging Software (Imaris, Oxford instruments, UK). Some of the images from Andor Dragonfly microscope were taken by Kruno Vukušić.

## **2.11. Image and data analysis**

All image analysis was done in ImageJ program (National Institute of Health, Bethesda, MD, SAD) and Imaris Viewer software (Imaris, Oxford Instruments, UK). ImageJ is a specialized open-source software for processing images obtained from a microscope. MatLab software (The MathWorks Inc., USA, R2018a) was used for data quantification and acquiring diagrams. Schemes were made in BioRender software. The estimation of significance of results was performed doing two-sample t-test. It produces “p-value” which determines the significance of



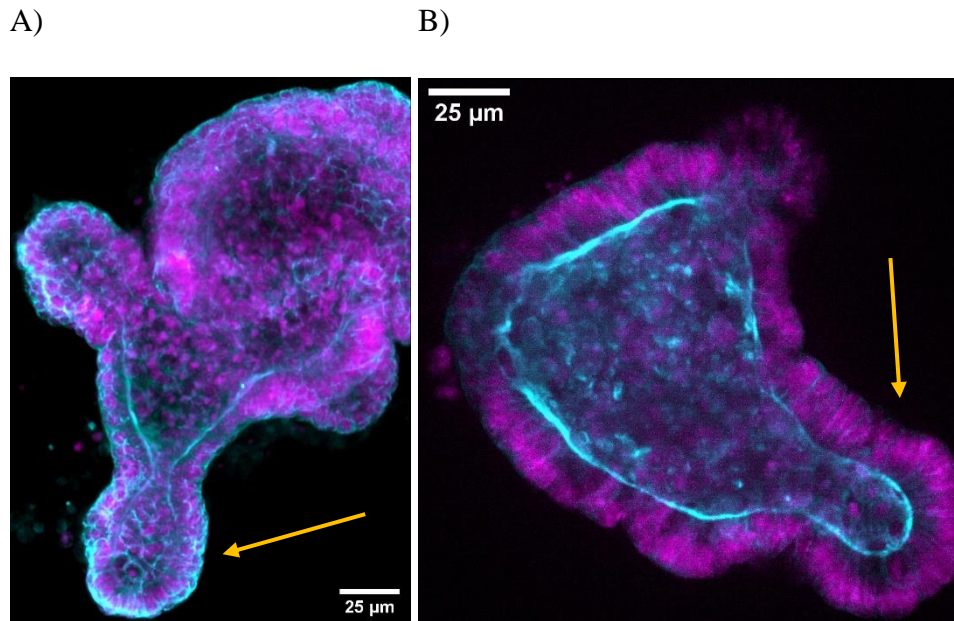


**Figure 22. Morphology of differentiated small intestine organoids.** The differentiated small intestine organoids have more budding structures (yellow arrow) and branch-like shape. DNA is stained with DAPI (1:1000, magenta) and actin is stained with Phalloidin (1:200, cyan).

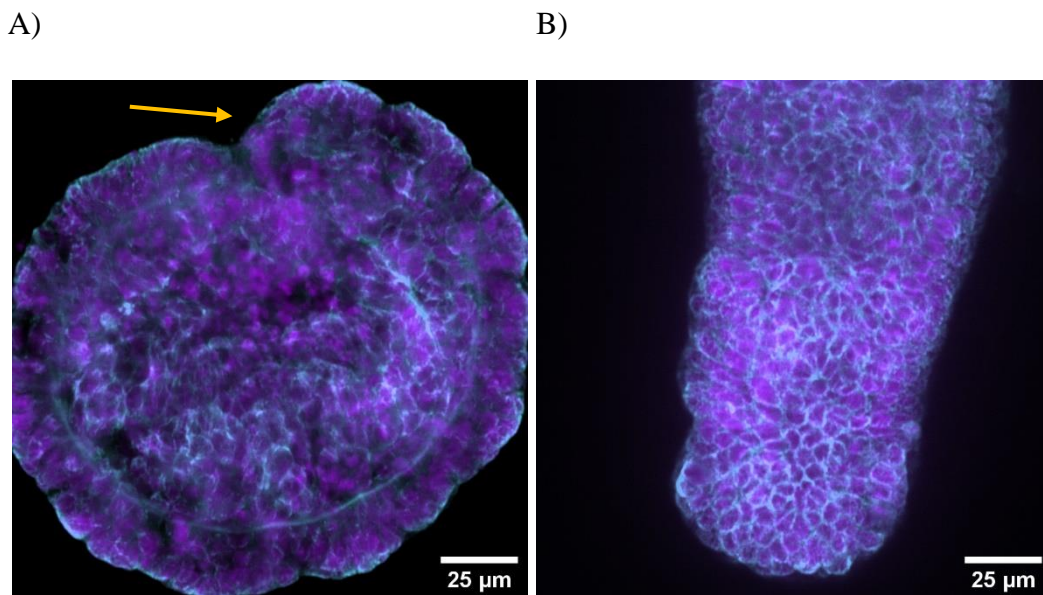


**Figure 23. Morphology of organoids starting to differentiate.** Organoids which are in between maintaining high proliferation and starting to rapidly differentiate have somewhat simpler structures with arising buds (yellow arrow). DNA is stained with DAPI (1:1000, magenta) and actin is stained with Phalloidin (1:200, cyan).

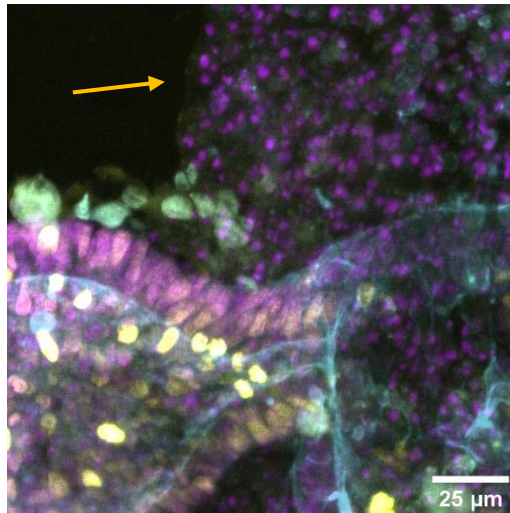


**Figure 24. Apoptotic cells surrounding the organoids.** When cells rapidly die in organoids, they tend to surround it (yellow arrow). They lose their typical structure and reduce in size. DNA is stained with DAPI (1:1000, magenta), actin is stained with Phalloidin (1:200, cyan), and proliferative cells are stained with Ki-67 antibody, cell proliferation marker (1:500, yellow).

### 2.13. Cell size measurements

To define the length and width of single cells in small intestine organoids, *Line* tool in ImageJ software is used. Only middle plane is taken when measuring cell length and width (figure 25). A line is drawn from the one end of the cell to border with another, while the ends are marked with phalloidin, marking the distribution of F-actin in cells. The same protocol is done two times, to measure length and width of the cells (figure 26).

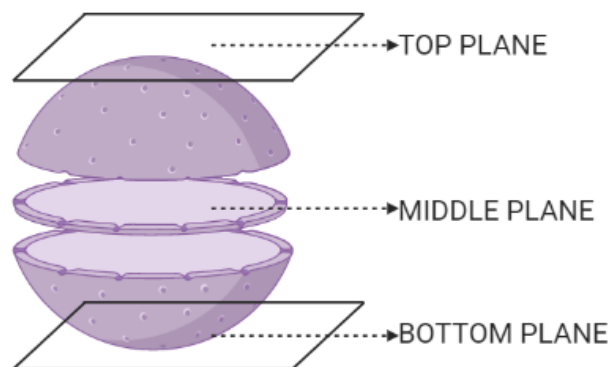


**Figure 25. Microscope images divided in stacks.** When obtaining images from a confocal microscope, they are divided into Z-stacks which combined give a 3D representation of the specimen. Only middle plane or Z-stack was taken to measure cell size and width.



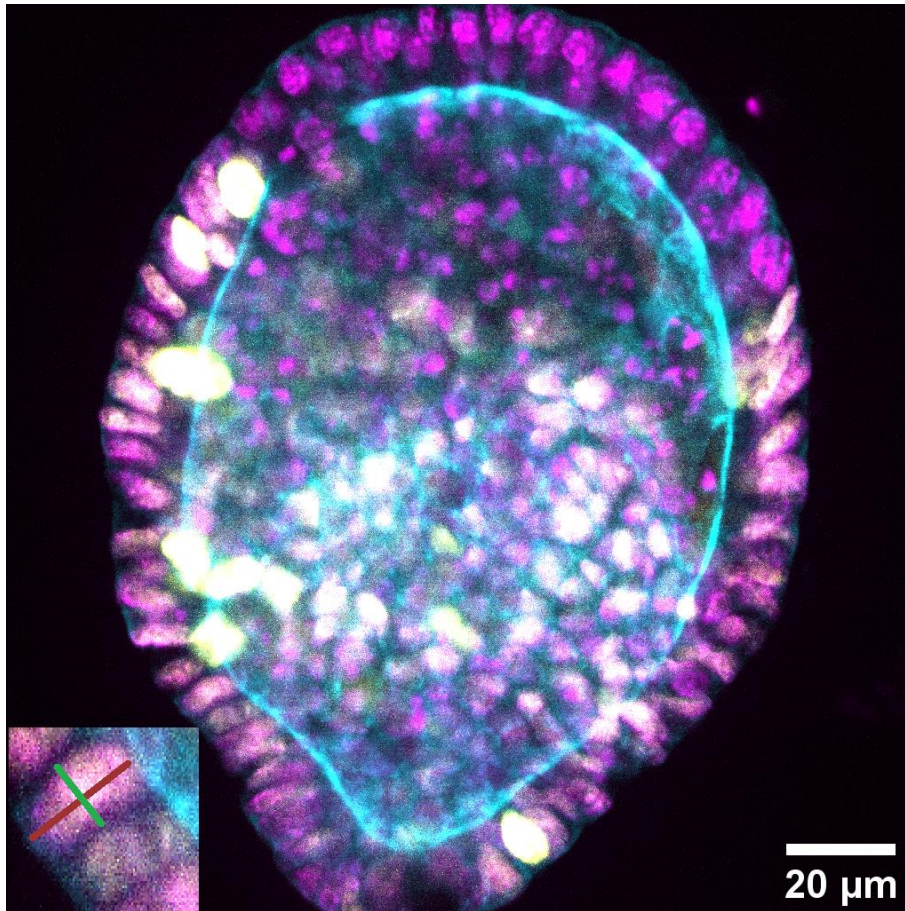


**Figure 26. Measuring cell size.** A line (red line) was drawn using *Line* tool in ImageJ on the longer axis of the organoid to determine the length of the cells in organoids. *Measure* tool was used to measure its length. When determining the width of the cells, a line (green line) was drawn along the shorter axis of the cell. DNA is stained with DAPI (1:1000, green), actin is stained with Phalloidin (1:200, red), and proliferative cells are stained with Ki-67 antibody (1:500, yellow). Insert shows bigger picture of cells in mouse small intestine organoid.

#### **2.14. Cell proliferation determination**

Cells were immunolabeled with proliferation marker Ki-67. Therefore, the cells stained with Ki-67 were determined as proliferating ones, whereas cells which were lacking Ki-67 marker were marked as resting cells in G0 phase (figure 27, 28, and 29).

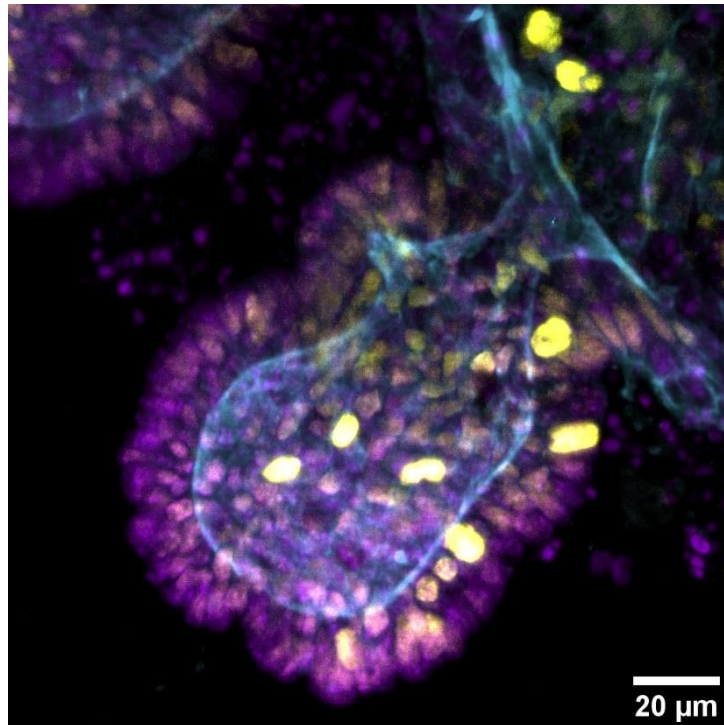


**Figure 27. Determining the proliferation rate of the organoids.** Cells containing the proliferation marker Ki-67 antibody (1:500, yellow) were counted and their number was divided with the number of cells in the whole organoids (magenta). DNA is stained with DAPI (1:1000, magenta) and actin is stained with Phalloidin (1:200, cyan).

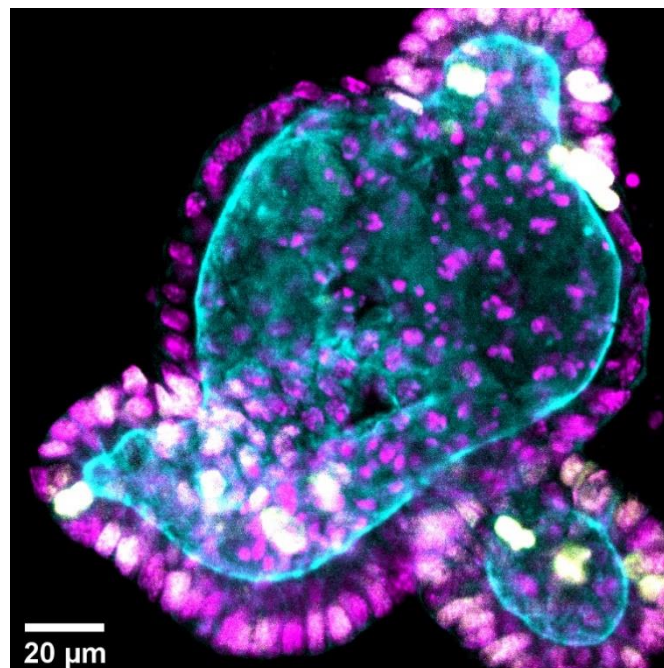


**Figure 28. Proliferating cells in mouse small intestine organoids.** Number of proliferative cells labeled with Ki-67 antibody (1:500, yellow) varies between different organoids. DNA is stained with DAPI (1:1000, magenta) and actin is stained with Phalloidin (1:200, cyan).

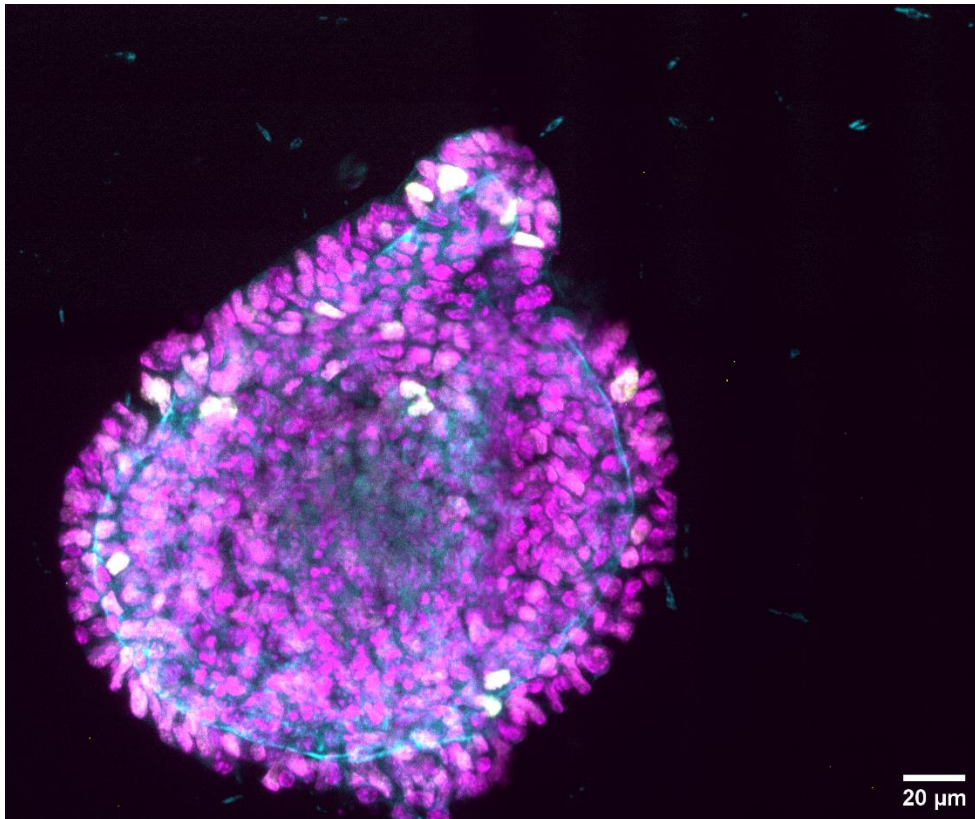


**Figure 29. Cell proliferation in mouse small intestine organoids.** Yellow cells labeled with Ki-67 antibody (1:500) represent proliferating cells viewed from the top plane. DNA is stained with DAPI (1:1000, magenta) and actin is stained with Phalloidin (1:200, cyan).

## Results

In the result section I will describe three experiments with cryovials containing mouse small intestine organoids and three experiments with mice. All the results of bio-imaging come from the third attempt of crypt isolation from a mouse.

### 3.1.1. Cryovial 1

Small intestine organoids were thawed, but after spinning them down, there was no visible pellet. However, small amount of remaining liquid was plated in Matrigel. No organoids were seen under the microscope in next 7 days. The color of the medium in the first cryovial was red.

### 3.1.2. Cryovial 2

The color of the medium in the second cryovial was red. Small intestine organoids were successfully plated on a prewarmed 24-well plate. However, they did not grow and after 3 days they started snapping (figure 30). Snapping happens because of the osmotic dysregulation in organoids and is characterized by mushroom like structures which have arms extending from the organoid. Main characteristic of this structures is their lack of an envelope which usually surrounds the cells in the mouse small intestine organoid.



**Figure 30. The growth of the small intestine organoids from a cryovial.** After seeding mouse small intestine organoids, they did not grow. After only three days they started rupturing (day 3). Scale bar is 50  $\mu\text{m}$ .

### 3.1.3. Cryovial 3

The color of the medium in the third cryovial was yellow. Small intestine organoids were efficiently plated on a prewarmed 24-well plate. Nonetheless, they looked the same as the days passed. After nine days in culture, they looked about the same as the first day in culture (figure 31). Sum of the three experiment attempts is given in table 5.

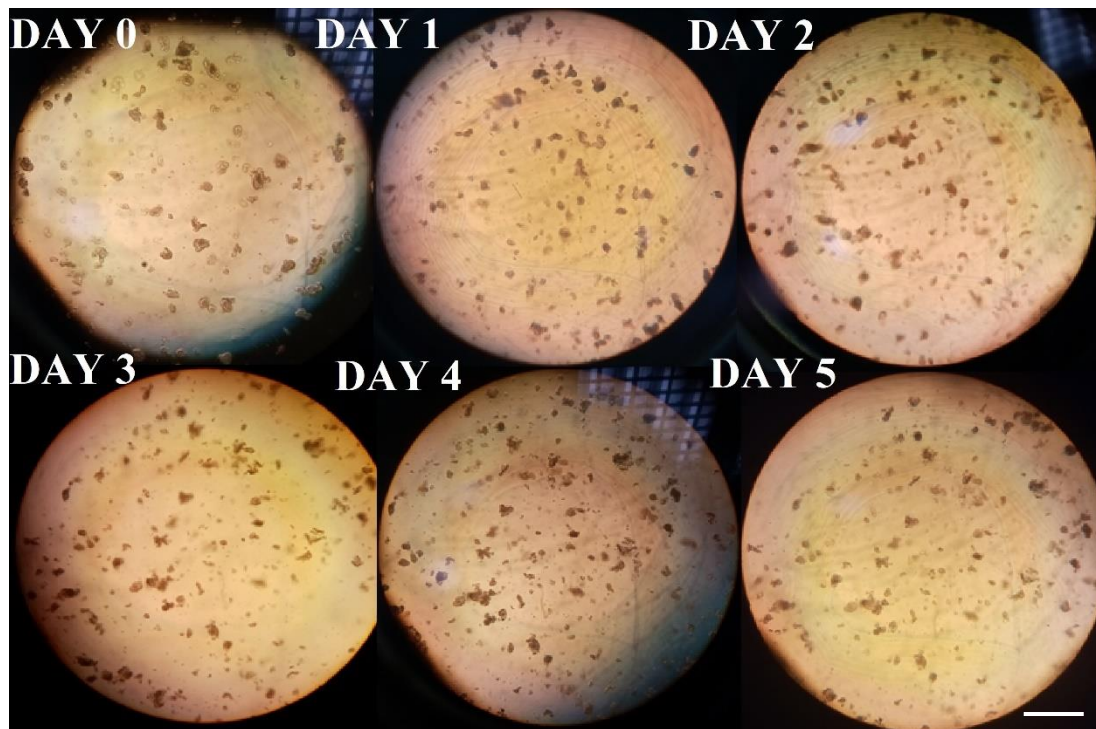


**Figure 31. Development of the mouse small intestine organoids.** The organoids remained almost the same size through five days of their development in culture. There were no signs of death like rupturing, but they also did not differentiate like normal mouse small intestine organoids. Scale bar is 100  $\mu\text{m}$ .

**Table 5. Results from three different cryovial thawing.**

	<b>Cystic organoids</b>	<b>Differentiated organoids</b>
<b>Cryovial 1</b>	✘	✘
<b>Cryovial 2</b>	✘	✘
<b>Cryovial 3</b>	✘	+

In summary, in the first two attempts no cystic neither differentiated organoids appeared. In the third attempt, there were some differentiated organoids, yet they did not grow.

### 3.2.1. Mouse 1

Mouse was male C57BL/6N, 6 weeks old. He weighed 19,2 g.

In the first attempt crypts isolation was done successfully. Many crypts were isolated from the small intestine and seeded on a preheated 24-well plate in a drop of Matrigel. However, after seeding them, crypts did not make any cystic or spherical organoids. They did not grow at all.

### 3.2.2. Mouse 2

Mouse was male C57BL/6N, 3 weeks old. He weighed 14,5 g.

In the second experiment crypt isolation was again very successful, but after seeding them on a preheated 24-well plate they started developing. After a day they have already grown into nicely shaped cystic organoids. However, after removing the medium with Wnt3a and Y-27632, organoids began to die instead of forming branched small intestine organoids (figure 32).

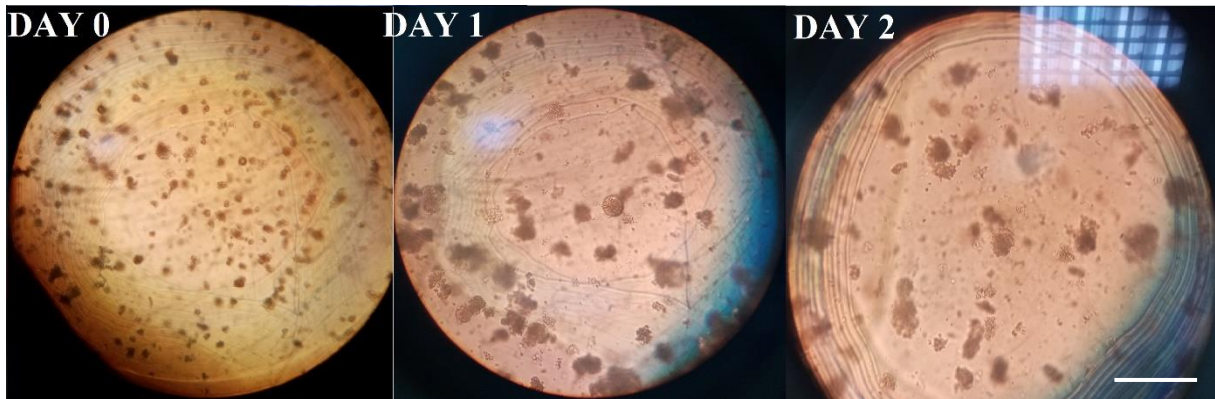


**Figure 32. Growth of the mouse small intestine organoids.** After a successful crypt isolation, some cystic, round organoids were formed, yet they all showed signs of rupturing (arrow) on the second day after isolation. Scale bar is 50  $\mu$ m.

### 3.2.3. Mouse 3

Mouse was female C57BL/6J, 5 weeks old. She weighed 17,2 g.

In the last try crypt isolation was less efficient. There were still enough of crypts to proceed with the experiment, but considerably less than in any of previous attempts. Crypts developed as expected, gave lots of cystic organoids in the first two days. After changing the medium to ICM, cystic organoids became differentiated and continue to grow (figure 33). Sum of the three experiments is given in Table 6.

**Table 6. The summary of the results from a mouse.**

	<b>Crypt formation</b>	<b>Cystic organoids</b>	<b>Differentiated organoids</b>
<b>Mouse 1</b>	+	×	×
<b>Mouse 2</b>	+	+	×
<b>Mouse 3</b>	+	+	+

In conclusion, in every case nicely shaped crypts were found and cultured, yet in the first attempt they did not give rise to any cystic or differentiated organoids. In the second attempt,

cystic organoids were formed on the second day, however, they did not start to differentiate after removing Wnt-3A from the medium. Lastly, in the third attempt, every step of the protocol was successful.

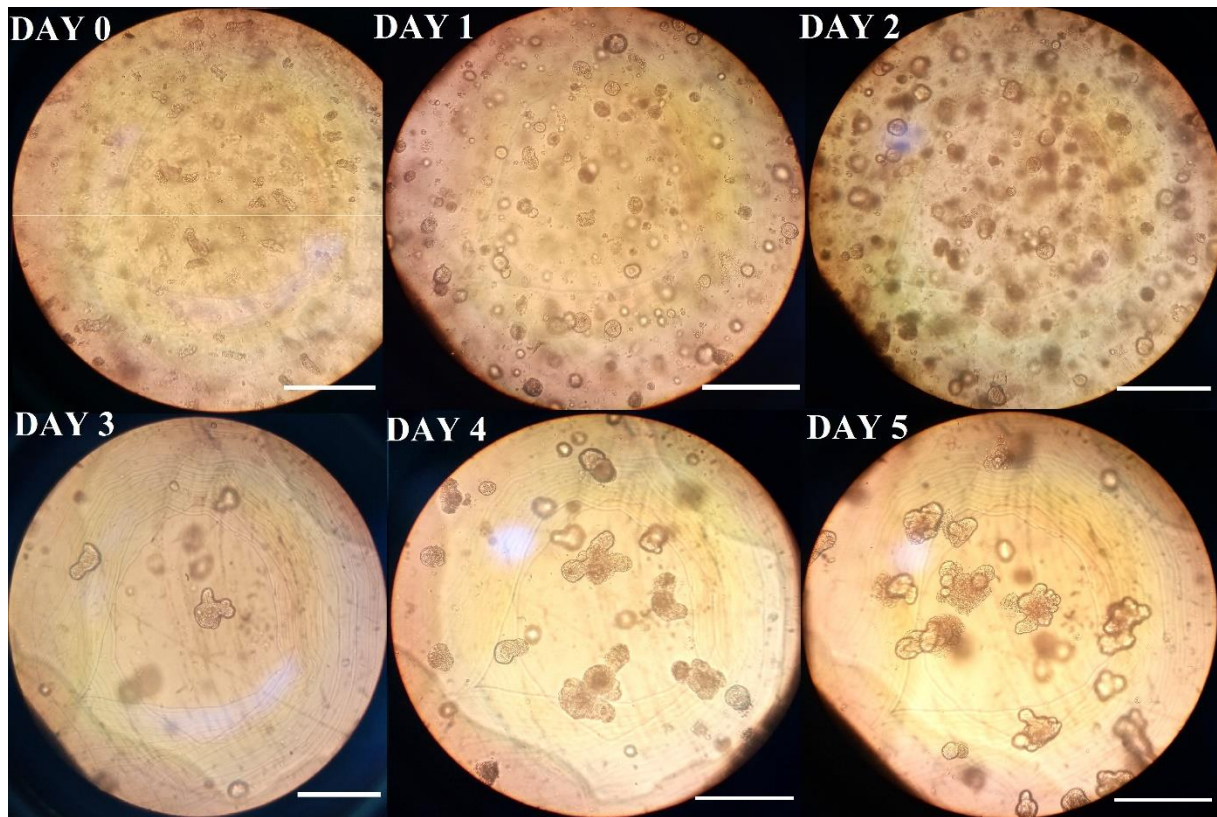


**Figure 33. The growth of mouse small intestine organoids.** After a successful crypt isolation (day 0), cystic organoids started to arise (day 2). On the third day they started to differentiate, and completely mimicked the small intestine morphology on the fifth day. Scale bar is 50  $\mu\text{m}$ .

### 3.3. Efficiency of immunolabeling

DAPI and Phalloidin staining was done successfully on the small intestine organoids, as DAPI stained blue the DNA in single cells and Phalloidin stained green (488 nm) F-actin in single cells (figure 34 and 35).

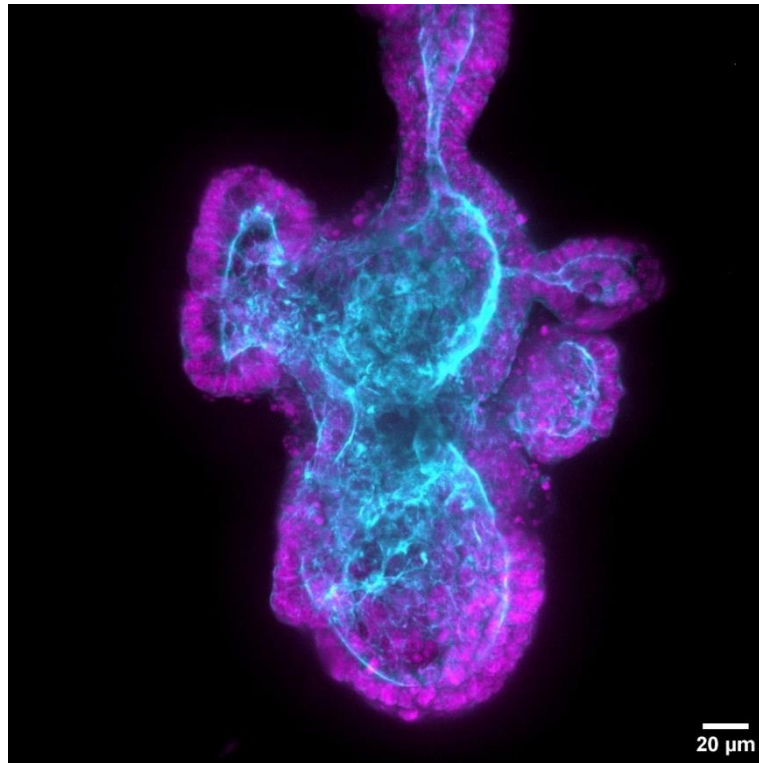


**Figure 34. Representation of a differentiated mouse small intestine organoid.** A differentiated mouse small intestine organoid with a few growing buds. DNA is labeled with DAPI (1:1000, magenta) and actin is labeled with Phalloidin (1:200, cyan).

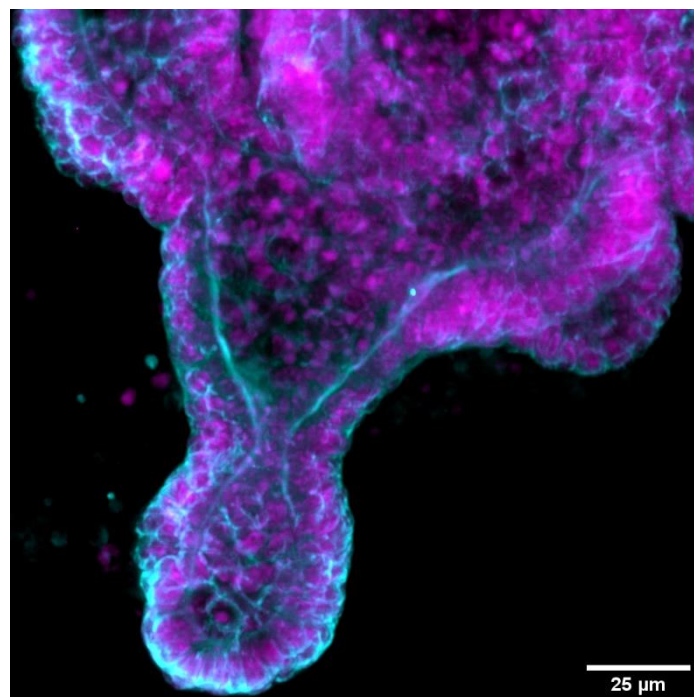


**Figure 35. A differentiated mouse small intestine organoid.** Branch-like structure of a differentiated mouse small intestine organoid. DNA is labeled with DAPI (1:1000, magenta) and actin is labeled with Phalloidin (1:200, cyan).



Immunolabeling small intestine organoids with tubulin antibody did not work so well. The antibody was stopped at the membranes of outer cells in the small intestine organoids and did not enter inner cells at all (figure 36). However, the antibody entered the dead cells surrounding some of the organoids.

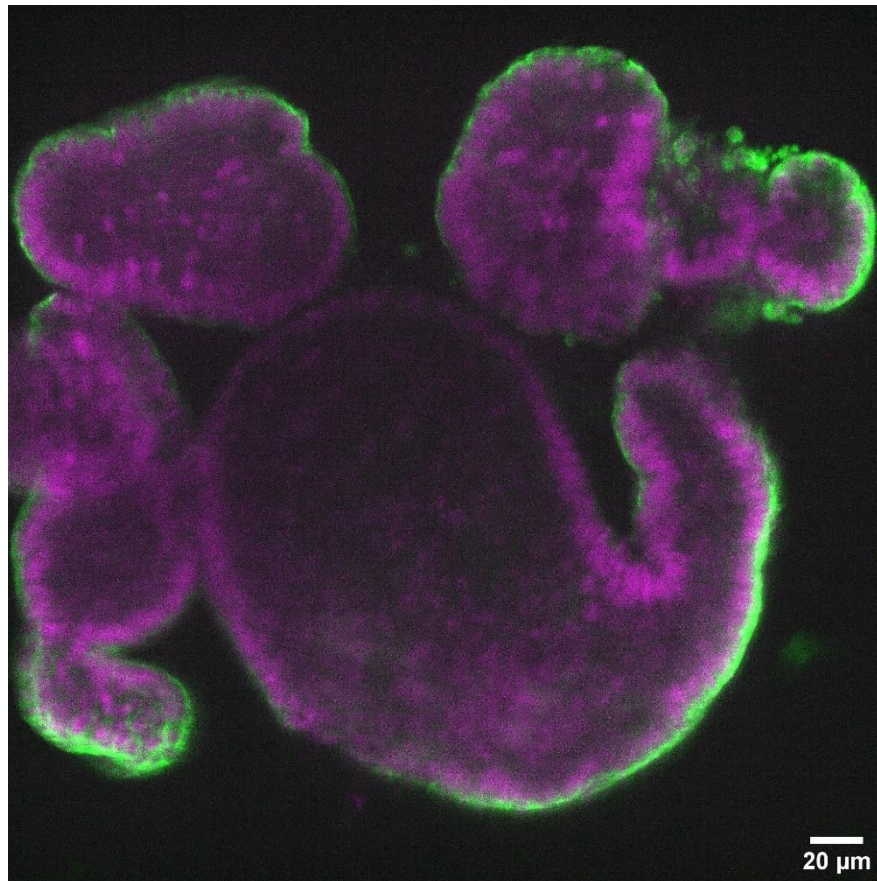


**Figure 36. A differentiating mouse small intestine organoid.** Mouse small intestine organoid in which DNA is labeled with DAPI (1:1000, magenta) and tubulin is labeled with antibodies (1:500, green). Tubulin did not enter the organoid and remained on the membranes.

However, immunostaining of the mouse small intestine organoids with antibody for proliferation marker Ki-67 was successfully done. The antibody for Ki-67 penetrated well inside the cells of the organoids, so all the proliferating cells chromosomes were marked with antibody for Ki-67 (figure 37 and 38).

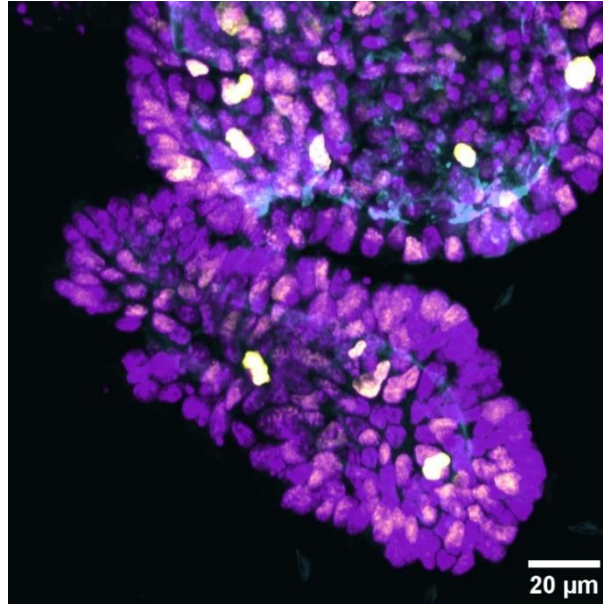


**Figure 37. A labeled mouse small intestine organoid.** A representation of a successful antibody penetration of Ki-67 antibody (1:500, yellow). DNA is labeled with DAPI (1:1000, magenta) and actin is labeled with Phalloidin (1:200, cyan).

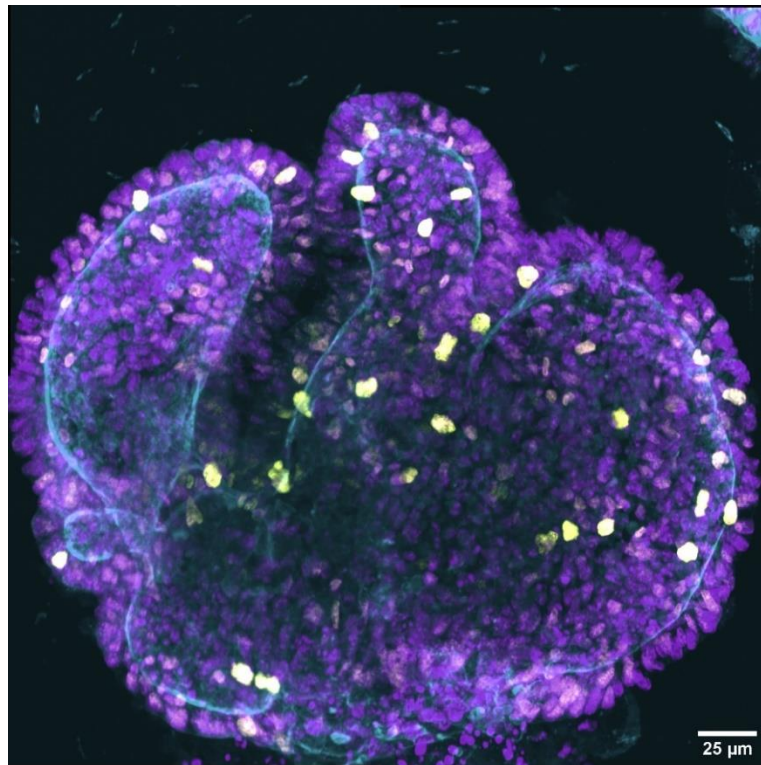


**Figure 38. Proliferation of mouse small intestine organoid.** Successful antibody staining of mouse small intestine organoid showed proliferating cells (yellow) labeled with Ki-67 antibody (1:500). DNA is labeled with DAPI (1:1000, magenta) and actin is labeled with Phalloidin (1:200, cyan).

### 3.4. Different morphology of the mouse small intestine organoids

When growing mouse small intestine organoids, they are recognized due to their specific morphological characteristics. Some of them tend to be roundly shaped and cystic, while others differentiate more towards the branching structures, full of new budding arms. However, some of them grow to have many budding structures, whereas others remain with only a few branch-like structures (figure 39). There are also organoids which are just starting to differentiate (figure 40).

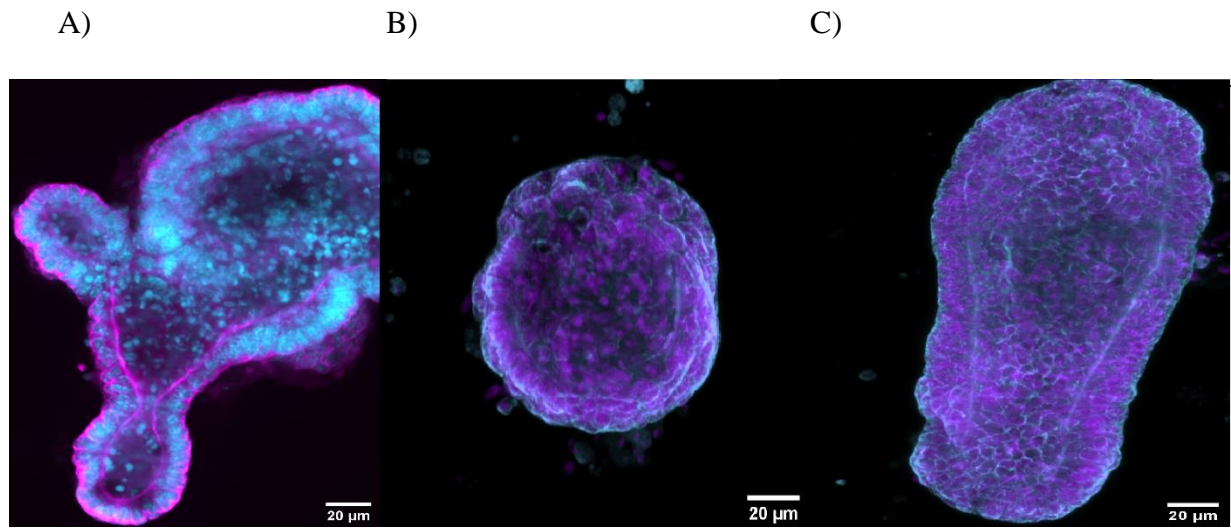


**Figure 39. Different structures of mouse small intestine organoids.** Mouse small intestine organoids can grow to become differentiated, branch-like structures (A), or be round, cystic organoids (B). However, organoids can also be in a state between two previously described, being long, but round and not fully differentiated (C). DNA is labeled with DAPI (1:1000, cyan in A; magenta in B and C) and actin is labeled with Phalloidin (1:200, magenta in A; cyan in B and C).

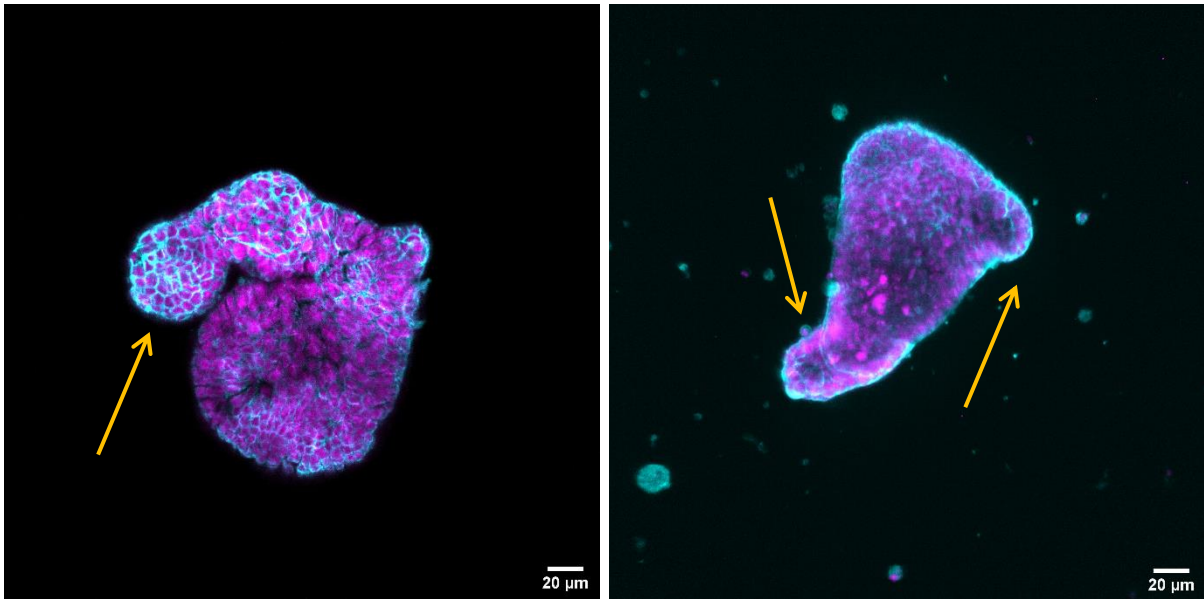


**Figure 40. Morphology of mouse small intestine organoids.** When mouse small intestine organoids start to differentiate, they change their morphology from cystic to more branched. The transition state is shown here where smaller branches start to appear (yellow arrow). DNA is stained with DAPI (1:1000, magenta) and actin is stained with Phalloidin (1:200, cyan).

### **3.5. Small intestine is a hollow organ**

Hollow structure of small intestine organoids is noticed when looking at images at different heights. Enteroids are made of external cells that make a sheet which surrounds a hollow inside. The statement concerns both differentiating (figure 41) and undifferentiated, cystic organoids (figure 42). The same is seen in fully differentiated organoids (figure 43). However, these organoids turned out somewhat flattened (figure 44).

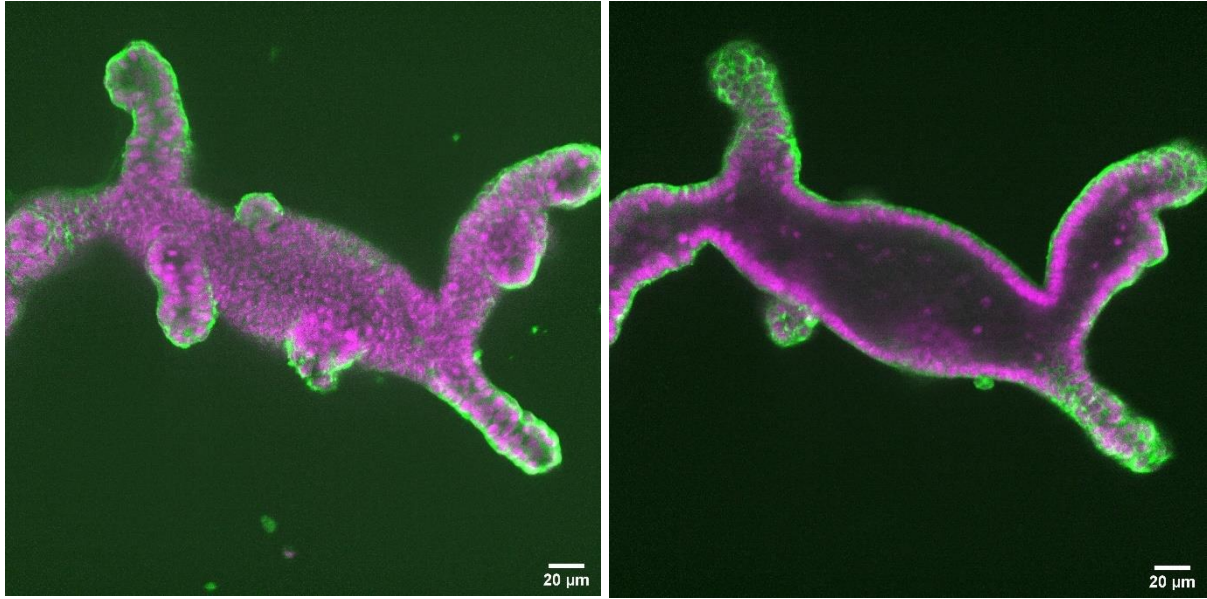


**Figure 41. A differentiated mouse small intestine organoid visualized from top and middle plane.** Mouse small intestine organoids are hollow structures (right picture) surrounded by a one cell layer (left picture). DNA is labeled with DAPI (1:1000, magenta) and tubulin is labeled with  $\alpha$ -tubulin antibody (1:500, green).

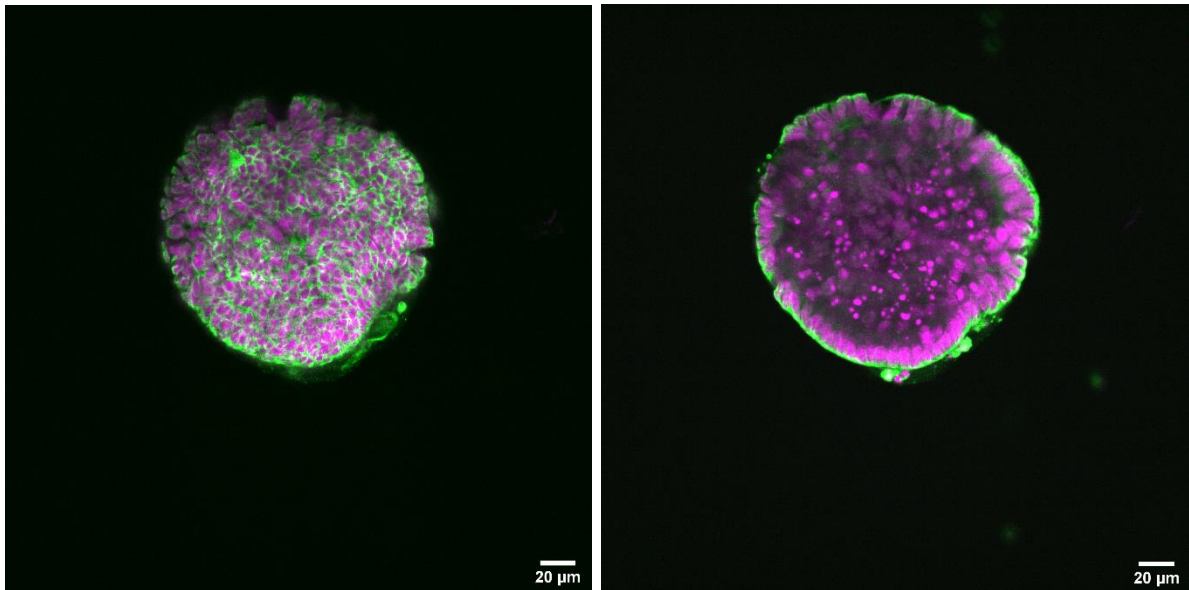


**Figure 42. A cystic mouse small intestine organoid visualized from top and middle plane.** Mouse small intestine organoids are hollow structures (right picture) which are surrounded by a one cell layer (left picture). DNA is labeled with DAPI (1:1000, magenta) and actin is labeled with  $\alpha$ -tubulin antibody (1:500, green).

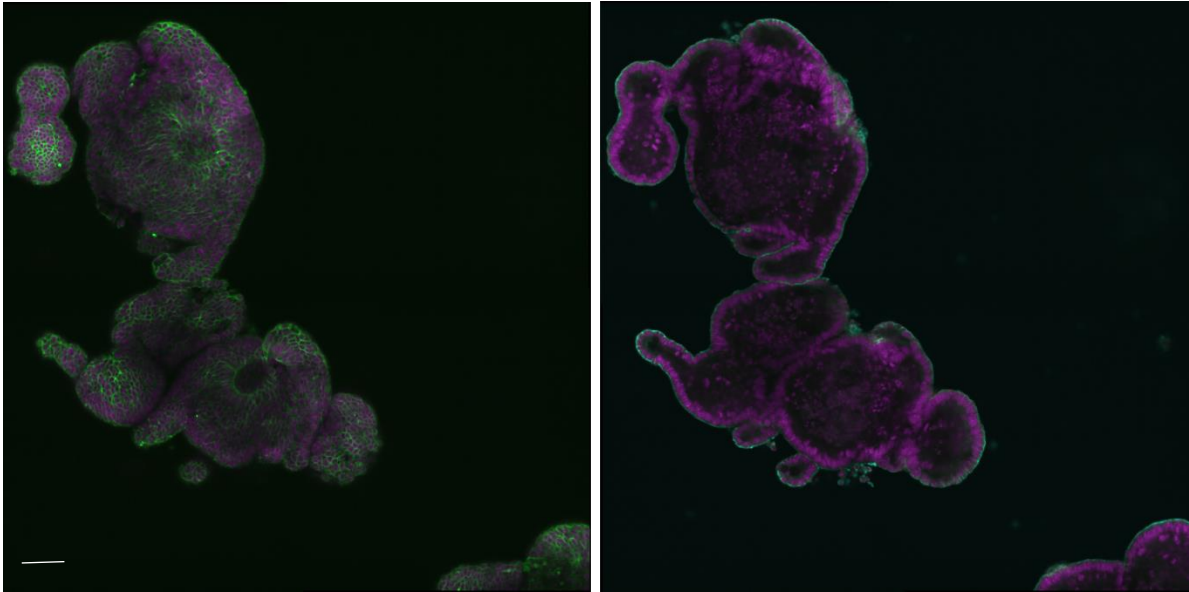


**Figure 43. Fully differentiated mouse small intestine organoid shown from top and middle plane.** Mouse small intestine organoids get their hollow structures early in cystic form and keep them until they are fully grown and differentiated. DNA is stained with DAPI (1:1000, magenta) and tubulin is labeled with  $\alpha$ -tubulin antibody (1:500, green). Scale bar is 50  $\mu$ m.

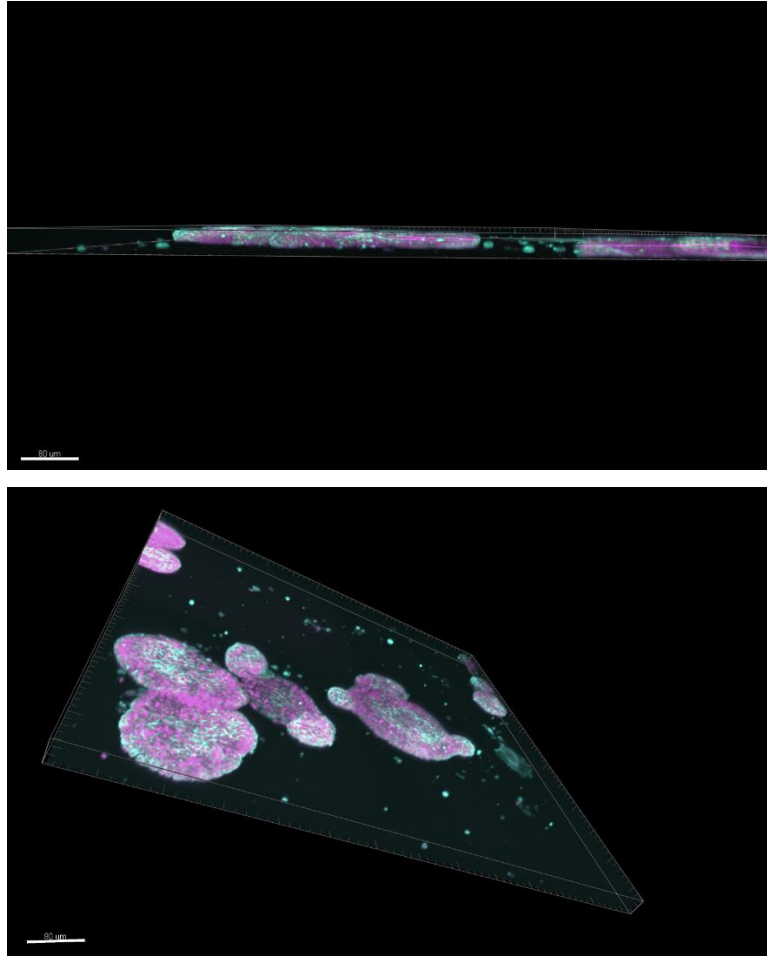


**Figure 44. 3D visualization of mouse small intestine organoids.** Due to technical disadvantages of the protocol, some of the small intestine organoids lose their volume and are therefore flattened. DNA is labeled with DAPI (1:1000, magenta) and actin is labeled with Phalloidin (1:200, cyan). Scale bar is 80 µm.

### **3.6. Cells vary in size in small intestine organoids**

Cell size is very different when looking at proliferating or non-proliferating cells. Therefore, cells in the small intestine organoids were classified as resting cells which lack Ki-67 marker, and proliferating cells which were stained with Ki-67 proliferation marker (figure 45). Other classification divided cells depending on their location as cells whose DNA is near the outer membrane of the small intestine organoid and cells whose DNA is away from the outer membrane of small intestine organoid.

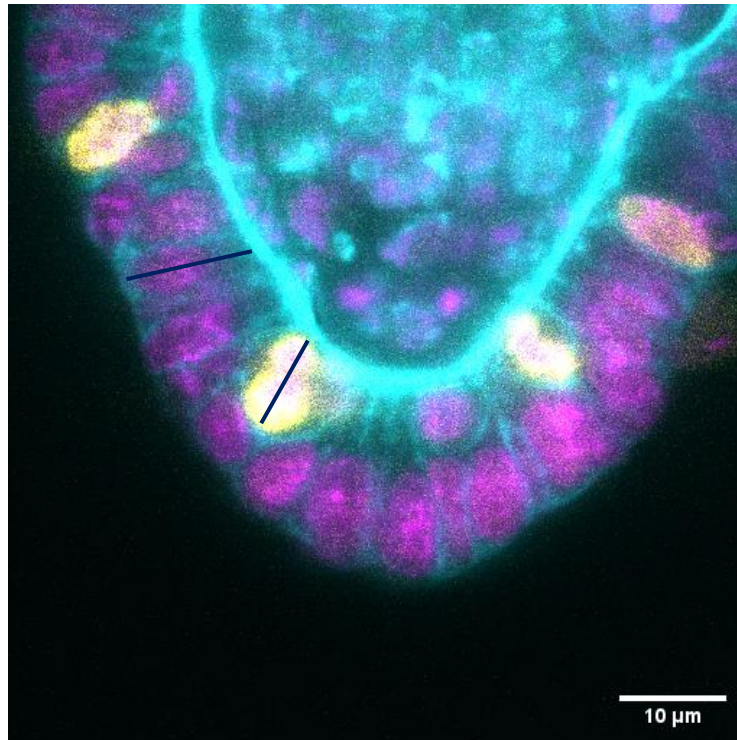


**Figure 45. A mouse small intestine organoid as viewed from the middle plane.** Appearance of the cells in the small intestine organoids from the middle plane. Cell lengths (blue line) are determined in proliferating (yellow) and resting cells (magenta). DNA is labeled with DAPI (1:1000, magenta), actin is labeled with Phalloidin (1:200, cyan), and proliferating cells are labeled with Ki-67 antibody (1:500, yellow).

Depending on the proliferation status and cell location, cell length greatly varies in the small intestine organoids (figure 46). A subpopulation of proliferating cells which is located closer to the outer membrane ( $6,201 \pm 0,094 \mu\text{m}$ ,  $n=5$ ), with their DNA touching the membrane is significantly smaller ( $p = 0,0001$ ) than proliferating cells whose DNA is away from that membrane ( $10,236 \pm 0,364 \mu\text{m}$ ,  $n=6$ ). However, the difference in length is not significant ( $p=0,3972$ ) between proliferating ( $6,201 \pm 0,094 \mu\text{m}$ ,  $n=5$ ) and resting, non-proliferating cells ( $5,812 \pm 0,423 \mu\text{m}$ ,  $n=5$ ) which are both located near the membrane. Yet, when comparing the length of the proliferating cells near the membrane ( $6,201 \pm 0,094 \mu\text{m}$ ,  $n=5$ ) and resting cells whose DNA is away from the membrane ( $13,228 \pm 0,446 \mu\text{m}$ ,  $n=8$ ), there is a significant difference ( $p < 0,0001$ ). This is also the case when comparing proliferating cells whose DNA is away from the membrane ( $10,236 \pm 0,364 \mu\text{m}$ ,  $n=6$ ) and resting cells whose DNA is near the membrane ( $5,812 \pm 0,423 \mu\text{m}$ ,  $n=5$ ;  $p < 0,0001$ ). There is also a significant difference ( $p = 0,0004$ ) between the length of proliferating ( $10,236 \pm 0,364 \mu\text{m}$ ,  $n=6$ ) and resting cells ( $13,228 \pm 0,446 \mu\text{m}$ ,  $n=8$ ) whose DNA is away from the membrane. When taking in consideration only



resting cells, they significantly differ ( $p < 0,0001$ ) in their length depending on the location of DNA near the membrane ( $5,812 \pm 0,423 \mu\text{m}$ ,  $n=5$ ) or away from the membrane ( $13,228 \pm 0,446 \mu\text{m}$ ,  $n=8$ ).

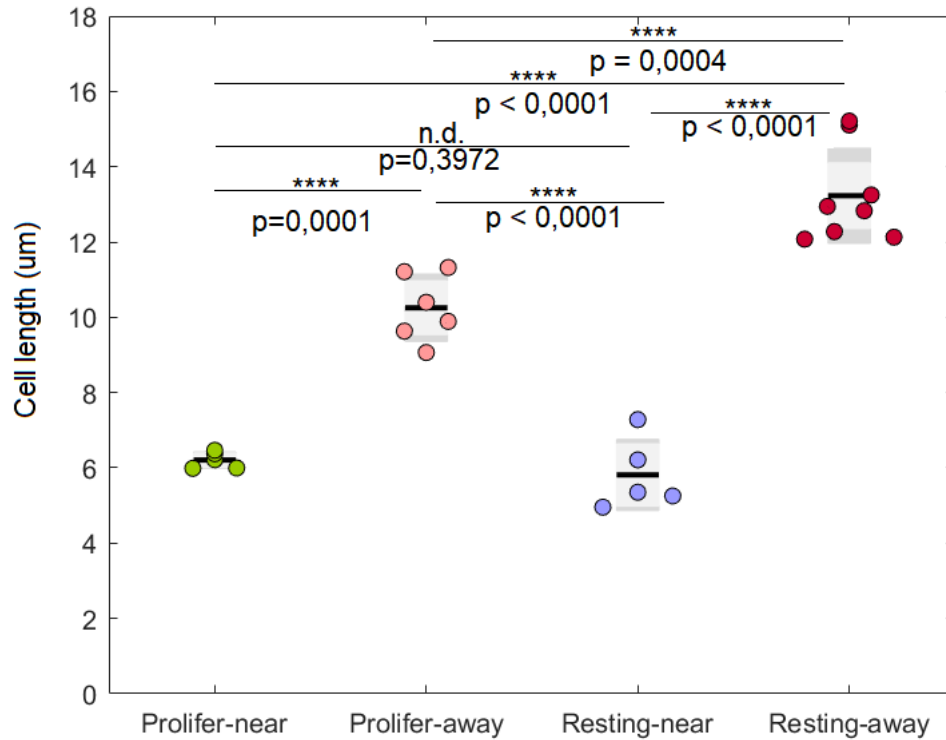


**Figure 46. Difference in the length of mouse small intestine organoid cells.** There is significant difference in the length of the proliferating cells whose DNA is near the membrane (Prolifer-near,  $6,201 \pm 0,094 \mu\text{m}$ ,  $n=5$ ), proliferating cells whose DNA is away from the membrane (Prolifer-away;  $10,236 \pm 0,364 \mu\text{m}$ ,  $n=6$ ), and resting cells whose DNA is away from the outer membrane of the small intestine organoids (Resting-away;  $13,228 \pm 0,446 \mu\text{m}$ ,  $n=8$ ). However, there is no significant difference ( $p = 0,3972$ ) between proliferating and resting cells whose DNA is near the outer membrane (Resting-near;  $5,812 \pm 0,423 \mu\text{m}$ ,  $n=5$ ) of small intestine organoids.

Width of the cells does not appear to be significantly different ( $p = 0,6747$ ) between proliferating cells whether their DNA is away ( $5,391 \pm 0,122 \mu\text{m}$ ,  $n=6$ ) or near the outer membrane ( $5,274 \pm 0,259 \mu\text{m}$ ,  $n=5$ ) of the small intestine organoids (figure 47), nor when comparing proliferating ( $5,274 \pm 0,259 \mu\text{m}$ ,  $n=5$ ) and resting cells whose DNA is near the outer membrane ( $5,285 \pm 0,461 \mu\text{m}$ ,  $n=5$ ) of the small intestine organoids ( $p = 0,9842$ ). Also, there was no significant difference ( $p = 0,8135$ ) between proliferating cells away from the membrane ( $5,391 \pm 0,122 \mu\text{m}$ ,  $n=6$ ) and resting cells whose DNA is near the membrane ( $5,285 \pm 0,461$

$\mu\text{m}$ ,  $n=5$ ). However, there is a significant difference ( $p = 0,0012$ ) between resting cells whose DNA is near the membrane ( $3,965 \pm 0,274 \mu\text{m}$ ,  $n=8$ ) and proliferating cells with the same location ( $5,391 \pm 0,122 \mu\text{m}$ ,  $n=6$ ) in the small intestine organoid. The same is true for the difference between resting cells whose DNA is away from the membrane ( $3,965 \pm 0,274 \mu\text{m}$ ,  $n=8$ ) compared to resting cells whose DNA is near the membrane ( $5,285 \pm 0,461 \mu\text{m}$ ,  $n=5$ ;  $p = 0,0229$ ) and to proliferating cells whose DNA is near the membrane ( $5,274 \pm 0,259 \mu\text{m}$ ,  $n=5$ ;  $p = 0,0079$ ).

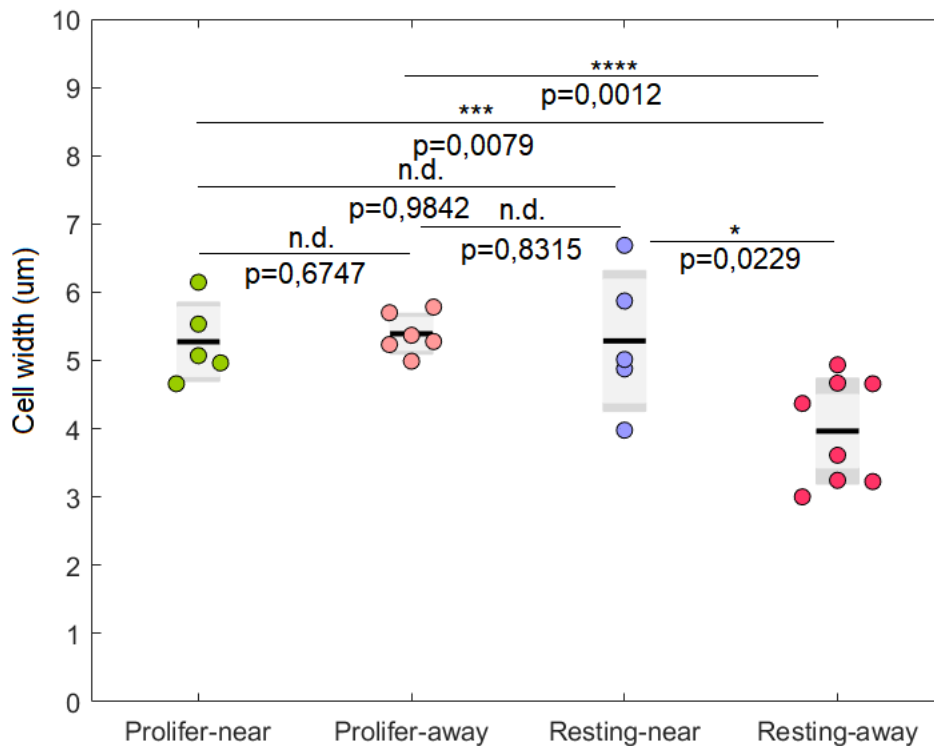


**Figure 47. Difference in the width of cells in mouse small intestine organoids.** There is no significant difference in the width of proliferating cells whose DNA is near (Prolifer-near;  $5,274 \pm 0,259 \mu\text{m}$ ,  $n=5$ ) or away (Prolifer-away;  $5,391 \pm 0,122 \mu\text{m}$ ,  $n=6$ ) from the outer membrane of the small intestine and resting cells whose DNA is near the membrane (Resting-near;  $5,285 \pm 0,461 \mu\text{m}$ ,  $n=5$ ). However, when compared with the width of resting cells whose DNA is away from the outer membrane (Resting-away;  $3,965 \pm 0,274 \mu\text{m}$ ,  $n=8$ ), there is significant difference ( $p = 0,0079$  for Prolifer-near;  $p = 0,0012$  for Prolifer-away;  $p = 0,0229$  for Resting-near).

### 3.7. Cell viability in small intestine organoids

An immunofluorescence assay was done to determine how the cells in the small intestine organoids grow and divide. Cells positively stained for proliferation marker Ki-67 were classified as proliferating cells, while the others were classified as resting cells (figure 48).

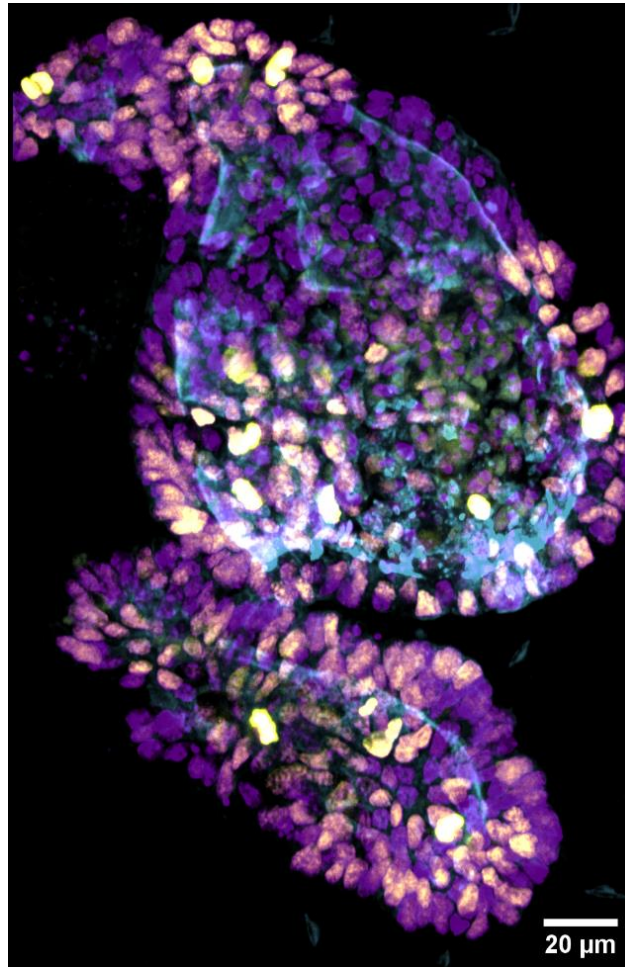


**Figure 48. Proliferative cells in culture.** Actively dividing cells in mouse small intestine organoids are stained with Ki-67 antibody (1:500, yellow). They are dispersed across the organoid. DNA is stained with DAPI (1:1000, magenta) and actin is stained with Phalloidin (1:200, cyan).

Overall proliferation rate of the bio-imaged small intestine organoids is 12,3%. Most of the cells (87,7%) are in the resting G0 phase of the cell cycle (figure 49).

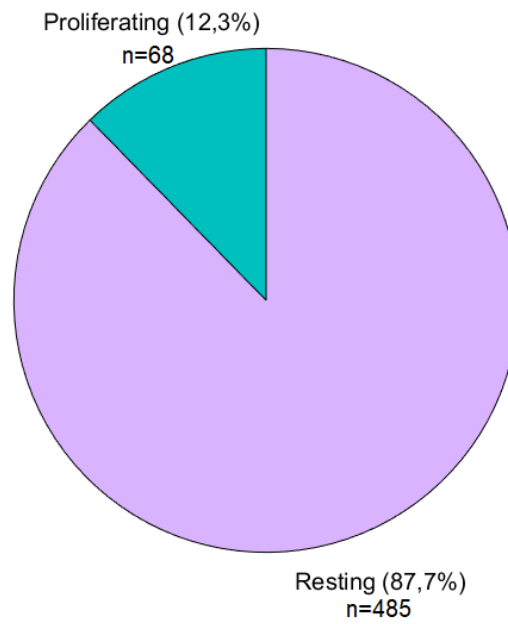


**Figure 49. Proliferation rate of mouse small intestine organoids.** Most of the cells in organoids were resting cells (87,7%; purple), while only a smaller portion of the cells were captured during the preparation to divide (12,3%; green).

However, when closely examined day by day, proliferation rate of the small intestine organoids shows a decrease when the organoids are older. Less cells were stained positive for Ki-67 when organoids that were already 5 days in culture were used than when freshly propagated organoids were immunoassayed (figure 50).

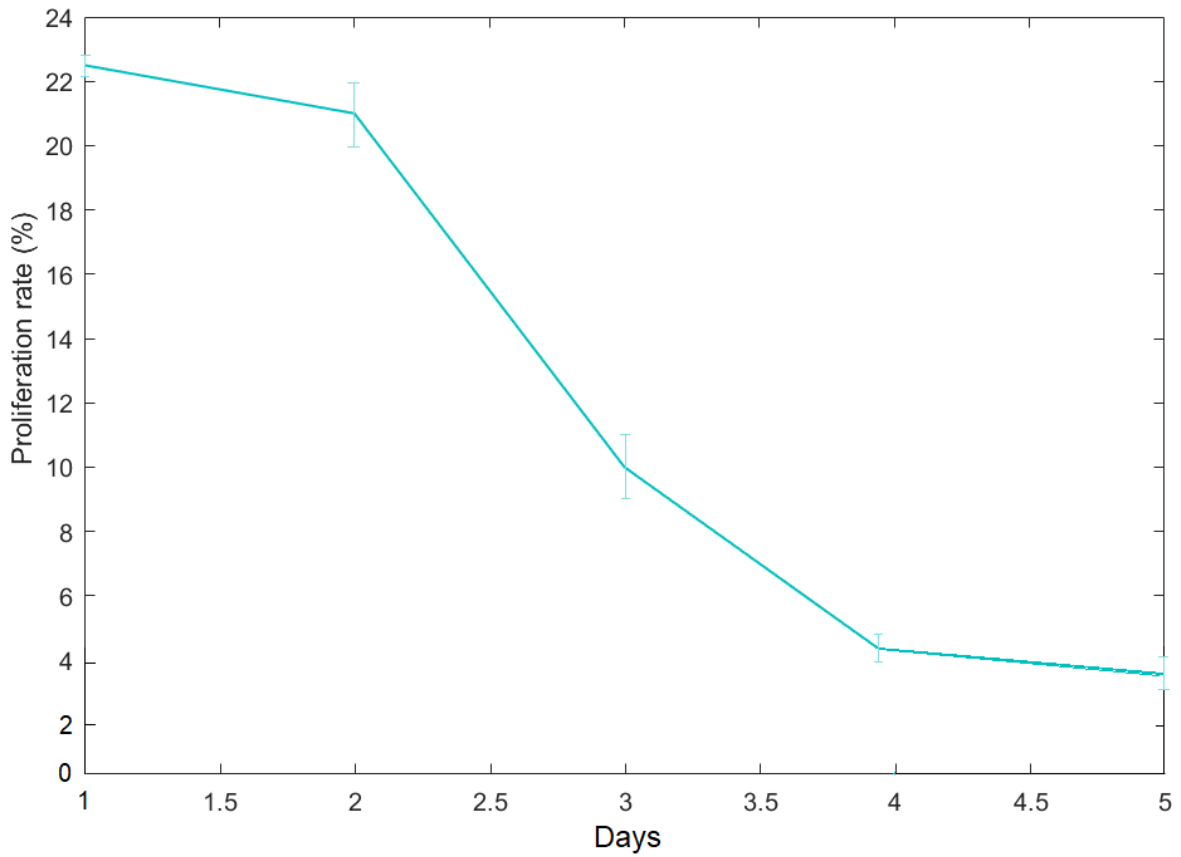


**Figure 50. Proliferation rate of mouse small intestine organoids depending on days already spent in culture.** The proliferation rate is at its highest when immunostaining was done on the first day after culture propagation and slowly decreases as older organoids were used.

## Discussion

To successfully establish and maintain an organoid culture it is crucial to optimize the growth medium. When there is even a minor disbalance in growth factors and signaling molecules, the organoids tend to grow slower, stop differentiating or worse, decaying and dying. The biggest problem in the first experiments was inaccurate concentration of R-spondin molecules which was added to the OBM. The first kit that we used contained the wrong instructions for making ICM, so the experiments were more successful in the second attempt with a different kit where the right concentration of R-spondin was listed. Since R-spondin is the key regulator of Wnt signaling pathway, organoids start to die when lacking R-spondin. It was clear that the deficiency in R-spondin caused organoids to stop growing and developing and finally resulted in organoids death. However, the abnormalities were first noticed only two days after starting to grow organoids, since the first two day the organoid culture medium is supplemented with recombinant Wnt3A protein. When Wnt3A protein is added to the culture, it drives the Wnt signaling pathway and there is no need for R-spondin molecules to inhibit the internalization of LRP6 receptors, at least for the first two days. Afterwards, the Paneth cells in the crypts of the small intestine start to produce their own Wnt molecules, so no further adding of the recombinant Wnt3A protein is needed. Since in the first steps of establishing an organoid culture, whether directly from a mouse or cryovials, cells go through a noticeable amount of stress, a rho-kinase inhibitor Y-27632 is added. If it is being omitted from the organoid growth medium, most of the organoids die from apoptosis (Levin et al., 2020).

An important step in propagation of organoids is removal of the old Matrigel which is done in the step of centrifugation. This step remained a critical one in every experiment done with the organoids. Suggested literature centrifuge speed is 300-400 rcf, but that speed was never big enough to pellet the organoids. The speed was adjusted to 500 or 600 rcf and gave results only after 5 min centrifugation at the speed of 500 rcf. Sometimes the speed had to be 700 rcf to give any pellet to propagate the organoids. Although the literature suggests that those speeds would destroy and kill organoids, the cells remained viable and organoids continued to grow and differentiate after splitting for weeks and months (Mahe et al., 2013). It is also important to use swinging bucket type of centrifuge instead of fixed angle centrifuge. The swinging bucket centrifuge allows the tubes to position horizontally against the center of the centrifuge which prevents the pellet from dispersing once the rotation is done. It is the type adjusted for cell biology, while the fixed angle centrifuge is specialized in small molecules biology, used for pelleting of proteins and similar molecules. The probable reason why thawing of the first

cryovial did not give any pellet of organoids is exactly the use of the wrong type of centrifuge. In the second attempt of thawing the cryovial, similar problem accrued. There was no pellet at the bottom of the tube, but a white cloud of organoids was seen floating within the tube. It was impossible to get it to the bottom of the tube, but I could not manage to remove the liquid media while maintaining most of the cloud of the organoids intact to dissolve them in Matrigel and plate them again. Regarding the speed of centrifugation, while risking the death of all the organoids with higher speeds, it prevented to lose all of them during supernatant removal. It was showed that organoids could resist higher speeds up to 700 rcf, whereas they were all lost while using the literature recommended speed of 300 rcf. Therefore, it was better to risk the death of the organoids instead of losing them in the supernatant.

Even though all the supplements were at the right concentration, thawing of the third cryovial did not work. While following the protocol for cryovial thawing and incubating it for a minute in water bath at 37 °C, the medium changed color to intense yellow, although the first two times it remained red. Since the frozen organoids were sent from the Netherlands, it is possible that something happened during the travel which caused them to die or it was just too stressful for them to survive. The yellow color suggested that something would be wrong with them and it was confirmed because they would not grow even after 7 days in culture. However, it is interesting that they did not show any obvious signs of snapping or dying like segmented structures, but they did not grow or differentiate. They seemed to look the same on the first and eighth day in culture. Unlike them, the organoids which died in the first attempts of direct isolation from mouse, which died because of the lack of R-spondin, have shown mushroom like segmented structures that have obviously snapped.

Despite the unsuccessful first two attempts of direct isolation of small intestine organoids from a mouse, the crypt isolation was noticeably better in those attempts than in the last, third try. The reason may be in the different strain of mice used. While in the first two attempts a male C57BL/6N mouse was used, in the last attempt organoids were isolated from a female C57BL/6J mouse. The main differences between two strains are metabolic mutations in C57BL/6J mouse. Those mutations are even more emphasized in female mice. When on high fat diet, these mice tend to develop obesity (Bryant, 2016). Furthermore, they were fed with high fat food in the laboratory before they were sacrificed. However, it was shown that for an increase in crypt density in the small intestine, it is better for mice to go through longer fasting periods (Mihaylova et al., 2019). Therefore, it would be better to sacrifice a C57BL/6N mouse in the next experiments.

It is very important to be careful during organoid propagation due to their sensitivity. If the organoids are mechanically too much dissolved prior to seeding which can happen if too many “ups and downs” are made with a pipette, they will form single cells. When single cells of an organoid are seeded, they tend to stop growing or grow much slower. This happens because organoids need inner cell contacts to fully grow and depend on the communication between cells. However, when organoids are not resuspended enough, the cells do not dissociate well, and they need to be splitted more often which is not preferable because the organoids are stressed more during the process. The stress can also cause them to stop growing after a while of the repeated process (O’ Rourke et al., 2016).

The protocol for immunostaining represents somehow modified protocol for seeding organoids and immunofluorescence staining of normal, 2D cell cultures. The main point of this upgraded protocol is to reduce the amount of Matrigel used, since it is a quite dense extracellular matrix alike hydrogel which limits the antibody penetration. It is known that Matrigel prevents antibodies from penetration towards the organoids and therefore causes non-specific staining throughout itself (Dekkers et al., 2019). To bypass this problem, organoids were not cultured as usual when prepared for immunostaining protocol. When propagating mouse small intestine organoids, they were seeded in a small drop of Matrigel, making them hardly accessible, surrounded with hydrogel from all the sides. However, this new method enables us to grow organoids close to the surface of a thin layer of Matrigel. While using this method, except for easier antibody penetration, a lot of Matrigel is spared. Basic principle of the protocol is firstly seeding a thin layer of Matrigel dissolved in the OBM which should be just enough to slightly cover the bottom of the well. It is important not to make the layer too thin because it could lead to formation of 2D culture of small intestine. When Matrigel is dissolved in the OBM and not seeded by itself as in normal propagation protocol, it does not solidify and allows post incubation entering of the organoids. However, they do not penetrate as deep as they would when directly dissolved in Matrigel. Moreover, it allows Matrigel to nicely spread across the bottom of the well while the excess OBM anyway evaporates and is removed while changing the medium. If the Matrigel is not dissolved well in the OBM it can form clumps on the bottom of the well which then contain all the organoids, but are more likely to be lost during the fixation step. The biggest problem with immunofluorescence staining of the organoids is the possibility to lose them while changing the solutions needed to fixate, permeabilize, stain and wash them. While using 4% paraformaldehyde, the structure of Matrigel can be disrupted and therefore



organoids are released in the paraformaldehyde which is washed out together with the organoids. However, using this method, most of the problem is solved.

Another big improvement in this method compared to the others developed for immunostaining of the organoids is shorter timescale needed to finish the protocol. The fixation periods are prolonged to overnight incubation in common protocols mostly because of the excess of Matrigel (Dekkers et al., 2019). While this protocol was developed to reduce the amount of Matrigel, the fixation period was also reduced to that of normal 2D cultures of 4-10 minutes. Moreover, duration of incubation with secondary antibody was also reduced from an overnight to only 2 hours incubation period. Overall process takes around two days less than most of the protocols which makes this protocol a lot less time consuming.

A problem that raised while developing this method was the flattening of the small intestine organoids. After all the steps done with coverslip which has organoids on it, the coverslip was put upside-down on a glass microscope slide. Due to a big pressure coming from the coverslip, most of the organoids were flattened to a different degree. To prevent this issue, a small piece of adhesive tape can be put on a glass microscope slide to prevent the coverslip from totally adhering to it (Dekkers et al., 2019). This way, a thin layer of air is left between the coverslip and glass microscope slide.

Efficacy of the staining's varied depending on the used antibody. Stainings without antibodies, with DNA stain DAPI and actin stain Phalloidin were mostly done successfully, meaning the shapes of DNA and actin in cells were nicely shown. While the concentration of mentioned stains remained constant, durations of different solution treatments were changed to reach a best solution. However, the efficiency of those staining did not depend on the duration of fixation or permeabilization.

Antibody staining was not as successful as above mentioned. When trying to visualize tubulin in small intestine organoids, the biggest problem was to get the tubulin antibody inside the cells. Instead of entering the organoids and its cells, tubulin antibody remained attached to the membranes of the cells. Although two different antibodies were used and the time of the fixation, permeabilization and incubation with antibodies were varied, none of the attempts worked. Another adjustment was a higher concentration of Triton X-100, the permeabilization reagent, but there was still no nice localization of the tubulin antibody. However, another problem may arise from the fact that anti-rat antibodies were used. Due to similarities between

mouse and rat antigens, a better solution would be to use antibodies from another, evolutionary more distinct species.

Since the immunostaining with Ki-67 antibodies worked better and the localization of the proliferation marker was consistent with literature, that validates the developed method. However, the question remains why it worked for Ki-67 antibody and did not for tubulin antibody.

Morphology of the mouse small intestine organoids changed during the experiment. First, they were rounder and more cystic, but when lacking Wnt3A they became differentiated, full of new buds and branches. Their behavior is therefore consistent with previously described organoids in publications. Another feature of the small intestine organoids is their cavity which represents the cavity in the physiological small intestine through which food passes during digestion. It is one of the evidences of similarity between organoids and native organs (Zietek and Rath, 2018).

Cell size in the mouse small intestine organoids vary depending on their proliferation status and location within the organoid. Length of the cells whose DNA is located away from the outer membrane of mouse small intestine organoids is longer, whether they are proliferating or not. When the cells get close to the outer membrane, they are smaller because they have just finished mitosis if they are not proliferating, meaning they lack Ki-67 marker; or because they are finishing mitosis at the moment, entering anaphase or telophase, if they are labeled with Ki-67 antibody. Their size and position are in consent with the orientation of cell division in the mouse small intestine organoids. When cells divide in the mouse small intestine organoids, two daughter cells move together towards the outer membrane of the small intestine organoid (figure 51). However, despite their differences, their size does not differ a lot from the primary intestinal epithelial cells (Fujimichi et al., 2019).

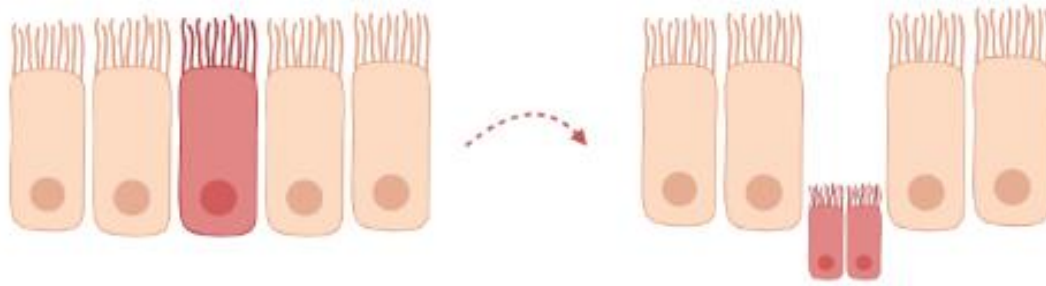


**Figure 51. The division of cells in mouse small intestine organoids.** When a cell divides in the mouse small intestine organoid, its two smaller daughter cells tend to go in a lower layer, closer to the outer membrane of mouse small intestine organoid. Red cell is entering mitosis.

The main characteristic of stem cells is their high proliferation rate. The proliferation rate must be higher than differentiation rate to maintain stemness of cells. However, in organoids differentiation rate slowly exceeds the proliferation rate which can be seen as budding structures appearing on small intestine organoids. It was shown here that proliferation in organoids slowly decreases as they are older which is in consent with previous experiments. The proliferation rate in my experiments with mouse small intestine organoids happens to be somewhat smaller than described in previous experiments (Carrol et al., 2018). This may be because lower rate of Ki-67 antibody penetration in organoids or their worse physiological state which causes them to stop dividing or divide slower.

## Conclusion

Analysis of confocal microscopy images of the mouse small intestine organoids showed that the optimization was successful and could be a routine protocol for establishing the organoids and their propagation in the lab. The most important steps in growing a culture of small intestine organoids are proper medium preparation and quick, yet careful handling of the organoids. The key is to apply just the right amount of the mechanical force to dissociate them, but not to make them single cells. The protocol could be applied for mouse colon organoids with minor changes in it.

The immunofluorescence assay on the mouse small intestine organoids culture works for some of the chosen antibodies, but needs major improvements for others. The duration of each step in the process is yet to be established more properly.

The characterization of organoid morphology revealed that the small intestine organoids are alike the native organ in their structure. A thin layer of cells surrounds a cavity in the inner organoid. Non differentiated organoids tend to be more roundly, cystically shaped, whereas the advanced differentiation leads to more branched structures full of new budding organoid arms.

The analysis of the cell size measured across the organoids indicated the presence of a population of a bigger non-dividing and dividing cells whose DNA is located away from the outer membrane, and smaller dividing and resting cells whose DNA is at the outer membrane of the mouse small intestine organoid. Their length was significantly different, while measuring the width showed only slight, nonsignificant changes.

The proliferation rate of the organoids decreased when organoids that were longer in culture were used, suggesting that increased differentiation interferes with maintenance of proliferation.

To conclude, a successful protocol optimization lead to the growth of fully differentiated, cystic and branch-like mouse small intestine organoids that showed normal small intestine morphology and a healthy proliferation rate when immunofluorescently stained.

## Literature

Bryant C. D. (2016): The blessings and curses of C57BL/6 substrains in mouse genetic studies. *Ann N Y Acad Sci.* **1245**: 31-33.

Carroll T. D., Newton I. P., Chen Y., Blow J. J., Nathke I. (2018): Lgr5+ intestinal stem cells reside in an unlicensed G1 phase. *J Cell Biol.* **217**: 1667-1685.

Chagastelles P. C., Nardi N. B. (2011): Biology of stem cells: an overview. *Kidney Int Suppl.* **1**: 63-67.

Clevers H. (2016): Modeling development and disease with organoids. *Cell.* **165**: 1586-1597.

Dekkers J. F., Alieva M., Wellens L. M., Ariese H. C. R., Jamieson P. R., Vonk A. M., Amatngalim G. D., Oost K. C., Snippert H. J. G., Beekman J. M., Wehrens E. J., Visvader J. E., Clevers H., Rios A. C. (2019): High-resolution 3D imaging of fixed and cleared organoids. *Nat Protoc.* **14**: 1756-1771.

Drost J., Clevers H. (2018): Organoids in cancer research. *Nat Rev Cancer.* **18**: 407-418.

Fujimichi Y., Otsuka K., Tomita M., Iwasaki T. (2019): An efficient intestinal organoid system of direct sorting to evaluate stem cell competition in vitro. *Sci Rep.* **9**: 20297.

Gehart H., Clevers H. (2019): Tales from the crypt: new insights into intestinal stem cells. *Nat Rev Gastroenterol Hepatol.* **16**: 19-34.

Hannelore D., Zietek T. (2015): Taste and move: glucose and peptide transporters in the gastrointestinal tract. *Exp Physiol.* **100**: 1441-1450.

Krausova M., Korinek V. (2014): Wnt signaling in adult intestinal stem cells and cancer. *Cell Signal.* **26**: 570-579.

Krzywinski M., Altman N. (2013): Significance, P values and t-tests. *Nature.* **10**: 1041-1042.

Lancaster M. A., Knoblich J. A. (2014): Organogenesis in a dish: modeling development and disease using organoid technologies. *Science.* **345**: 1247125.

Lancaster M. A., Renner M., Martin C. A., Wenzel D., Bicknell L. S., Hurles M. E., Homfray T., Penninger J. M., Jackson A. P., Knoblich J. A. (2013): Cerebral organoids model human brain development and microcephaly. *Nature.* **501**: 373-379.

Leung C. Tan S. H., Barker N. (2018): Recent advances in Lgr5+ stem cell research. *Trends Cell Biol.* **28**: 380-391.

Levin G., Zuber S. M., Squillaro A. I., Sogayar M. C., Grikscheit T. C., Carreira A. C. O. (2020): R-spondin 1 (RSPO1) increases mouse intestinal organoid unit size and survival *in vitro* and improves tissue-engineered small intestine formation *in vivo*. *Front Bioeng Biotechnol.* **8**: 476.

Lindberg K., Brown M. E., Chaves H. V., Kenyon K. R., Rheinwald J. G. (1993): In vitro propagation of human ocular surface epithelial cells for transplantation. *Invest Ophthalmol Vis. Sci.* **34**: 2672-2679.

Lucey B. P., Nelson-Rees W. A., Hutchins G. M. (2009): Henrietta Lacks, HeLa cells, and cell culture contamination. *Arch Pathol Lab Med.* **133**: 1463-1467.

Mahe M. M., Aihara E., Schumacher M. A., Zavros Y., Montrose M. H., Helmrath M. A., Sato T., Shroyer N. (2013): Establishment of gastrointestinal epithelial organoids. *Curr Protoc Mouse Biol.* **3**: 217-240.

Mihaylova M. M., Cheng C. W., Cao A. Q., Tripathi S., Mana M. D., Bauer-Rowe K. E., Abu-Remaileh M., Clavain L., Erdemir A., Lewis C. A., Freinkman E., Dickey A. S., La Spada A. R., Huang Y., Bell G. W., Deshpande V., Carmeliet P., Katajisto P., Sabatini D. M., Yilmaz O. H. (2019): Fasting activates fatty acid oxidation to enhance intestinal stem cell function during homeostasis and aging. *Cell Stem Cell.* **22**: 769-778.

Nishiyama K., Sugiyama M., Mukai T. (2016): Adhesion properties of lactic acid bacteria on intestinal mucin. *Microorganisms.* **4**: 34.

O' Rourke K. P., Ackerman S., Dow L. E., Lowe S. W. (2016): Isolation, culture, and maintenance of mouse small intestinal stem cells. *Bio Protoc.* **6**: e1733.

Rheinwald J. G., Green H. (1975): Serial cultivation of strains of human epidermal keratinocytes: the formation of keratinizing colonies from single cells. *Cell.* **6**: 331-343.

Sato T., Clevers H. (2015): SnapShot: growing organoids from stem cells. *Cell.* **161**: 1700-1701.

Sato T., Stange D. E., Ferrante M., Vries R. G. J., Van Es J. H., Van den Brink S., Van Houdt W. J., Pronk A., Van Gorp J., Siersema P. D., Clevers H. (2011): Long-term expansion of epithelial organoids from human colon, adenom, adenocarcinoma, and Barret's epithelium. *Gastroenterology.* **141**: 1762-1772.

- Sato T., Vries V. G. (2009): Single Lgr5 stem cells build crypt-villus structures in vitro without a mesenchymal niche. *Nature*. **459**: 262-265.
- Scholzen T., Gerdes J. (2000): The Ki-67 protein: from the known and the unknown. *J Cell Physiol*. **182**: 311-322.
- Shokryazdan P., Jahromi M. F., Liang J. B., Ramasamy K., Sieo C. C., Ho Y. W. (2017): Effects of lactobacillus salivarius mixture on preformance, intestinal health and serum lipids of broiler chickens. *PLoS One*. **12**: e0175959.
- Taciak B., Pruszyńska I., Kiraga L., Bialasek M., Krol M. (2018): Wnt signaling pathway in development and cancer. *J Physiol Pharmacol*. **69**.
- Van Barker N., Es J. H. (2007): Identification of stem cells in small intestine and colon by marker gene Lgr5. *Nature*. **449**: 1003-1007.
- Wallach T., Bayrer J. R. (2017): Intestinal organoids: new frontiers in the study of intestinal disease and physiology. *J Pediatr Gastroenterol Nutr*. **64**: 180-185.
- Wang J. Y., Liu Z. R., Ren M., Lin W. (2017): 2-benzothiazoleacetonitrile based two-photon fluorescent probe for hydrazine and its bio-imaging and environmental applications. *Sci Rep*. **7**: 1530.
- Włoga D., Joachimiak E., Fabczak H. (2017): Tubulin post-translational modifications and microtubule dynamics. *Int J Mol Sci*. **18**: 2207.
- Xia Y., Nivet E., Sancho-Martinez I., Gallegos T., Suzuki K., Okamura D., Wu M. Z., Dubova I., Rodriguez Esteban C., Montserrat N., Campistol J. M., Izpisua Belmonte J. C. (2013): Directed differentiation of human pluripotent cells to ureteric bud kidney progenitor-like cells. *Nat Cell Biol*. **15**: 1507-1512.
- Yoshikawa T., Inoue R., Matsumoto M., Yajima T., Ushida K., Iwanaga T. (2011): Comparative expression of hexose transporters (SGLT1, GLUT1, GLUT2 and GLUT5) throughout the mouse gastrointestinal tract. *Histochem Cell Biol*. **135**: 183-194.
- Zakrzewski W., Dobrzynski M., Szymonowicz M., Rybak Z. (2019): Stem cells: past, present, and future. *Stem Cell Res Ther*. **10**: 68.
- Zietek T., Rath E. (2018): Intestinal organoids: mini-guts grown in the laboratory. U: Davies J. A., Lawrence M. L. (ur.) *Organoids and mini-organs*. Academic Press, Elsevier Inc., 43-71.

## **Curriculum vitae**

### **Personal information:**

Snježana Kodba

15 February 1997

Čakovec, Croatia

### **Education:**

Undergraduate program in Molecular Biology, Department of Biology,

Faculty of Science, University of Zagreb, Zagreb (Croatia)

Gymnasium Josipa Slavenskog, Čakovec (Croatia)

### **Conferences:**

Risteski P., Kodba S., Pavin N., Tolić I. M.

Mitotic spindle: From living and synthetic systems to theory 2019,

Split (Croatia), poster presentation.

### **Science popularization:**

Summer Science Factory (LJTZ), 2016-2018, Split (Croatia)

Summer School of Science (S3), 2016-2019, Požega (Croatia)

Magic in Science, 2016-2019, Faculty of Science, University of Zagreb,

Zagreb (Croatia)

Night of Biology 2018, Faculty of Science, University of Zagreb,

Zagreb (Croatia)